

1 **Biogenically driven marine organic aerosol production over the West**  
2 **Pacific Ocean**

3 Yujue Wang<sup>1, 2, \*</sup>, Yizhe Yi<sup>1</sup>, Wei Xu<sup>3, \*</sup>, Yiwen Zhang<sup>1</sup>, Shubin Li<sup>1</sup>, Hong-Hai Zhang<sup>4</sup>, Mingliang Gu<sup>1</sup>,  
4 Shibo Yan<sup>5</sup>, Jialei Zhu<sup>6</sup>, Chao Zhang<sup>1, 2</sup>, Jinhui Shi<sup>1, 2</sup>, Yang Gao<sup>1, 2</sup>, Xiaohong Yao<sup>1, 2</sup>, Huiwang Gao<sup>1, 2</sup>

5 <sup>1</sup>Frontiers Science Center for Deep Ocean Multispheres and Earth System, Key Laboratory of Marine Environment and  
6 Ecology, Ministry of Education of China, Ocean University of China, Qingdao, China

7 <sup>2</sup>Laboratory for Marine Ecology and Environmental Science, Qingdao Marine Science and Technology Center, Qingdao,  
8 China

9 <sup>3</sup>State Key Laboratory of Advanced Environmental Technology, Institute of Urban Environment, Chinese Academy of  
10 Sciences, Xiamen, China

11 <sup>4</sup>Key Laboratory of Marine Chemistry Theory and Technology, Ministry of Education, Ocean University of China, Qingdao  
12 266100, China

13 <sup>5</sup>Third Institute of Oceanography, Ministry of Natural Resources, Siming District, Xiamen, Fujian 361005, China

14 <sup>6</sup>Institute of Surface-Earth System Science, School of Earth System Science, Tianjin University, Tianjin, China

15  
16 \* Correspondence to: Yujue Wang ([wangyujue@ouc.edu.cn](mailto:wangyujue@ouc.edu.cn)); Wei Xu ([wxu@iue.ac.cn](mailto:wxu@iue.ac.cn))  
17

18 **Abstract.** Marine organic aerosols play crucial roles in cloud formation and climate regulation within the marine boundary  
19 layer. However, the abundance of marine primary organic carbon (MPOC) generated by sea spray and secondary organic  
20 carbon (MSOC) formed via gas-to-particle conversion or atmospheric oxidation/aging processes remains poorly quantified,  
21 which hinders our understanding on the climate effects of marine aerosols. In this work, two shipboard cruises were  
22 conducted over the West Pacific Ocean to estimate abundance and compositions of marine organic aerosols. We propose an  
23 observation-based approach to quantify the MPOC and MSOC using a combined parameterization of the observed  $\text{Na}^+$  in  
24 fine aerosol particles and the surface chlorophyll-*a* (*Chl-a*), an indicator of marine biological activity. The parameterization  
25 approach of MPOC using  $[\text{Chl-a}] \times [\text{Na}^+]^{0.45}$  was validated through comparing with the water-insoluble organic carbon in the  
26 aerosol samples. The estimated MPOC ( $0.33 \pm 0.32 \mu\text{gC m}^{-3}$ ) averagely accounted for 56%–66% of the total organic carbon  
27 in the collected samples, which was mainly attributed to the protein-like substances transferred into the sea spray aerosols  
28 from seawater. Over the West Pacific Ocean, the MPOC and MSOC displayed peak concentrations over the regions 5°S–  
29 5°N ( $0.64 \pm 0.56$  and  $0.44 \pm 0.32 \mu\text{gC m}^{-3}$ ) and 35°N–40°N ( $0.46 \pm 0.35$  and  $0.51 \pm 0.30 \mu\text{gC m}^{-3}$ ). The variation and spatial  
30 distribution of MPOC and MSOC along the latitude were driven by the marine biological activities. High MSOC  
31 concentrations were also observed over the region of 15°N–20°N ( $0.35 \pm 0.41 \mu\text{gC m}^{-3}$ ), which was due to an additional  
32 contribution by the oxidation of volatile organic precursors from the photochemical production of seawater organics. This  
33 study proposes a parameterization approach to quantify the MPOC and MSOC over the Pacific Ocean or other oceanic areas.

34 Our results highlight the marine biogenically driven formation of marine organic aerosols, and different quantitative relations  
35 of MPOC with seawater *Chl-a* and other parameters are needed based on in-situ observations across oceanic regions.

36 **1 Introduction**

37 Marine aerosols are one of the most important natural aerosols on a global scale (De Leeuw et al., 2011; Quinn et al.,  
38 2015b). Observation and modeling studies have proved that marine aerosols are an important source of cloud condensation  
39 nuclei (CCN) and ice-nucleating particles (INPs) over remote oceanic areas, and play a vital role in Earth's radiation balance  
40 (Demott et al., 2016; Quinn et al., 2017; Sinclair et al., 2020; Vergara-Temprado et al., 2017; Wolf et al., 2019; Xu et al.,  
41 2022). Sea salt, sulfate, and organic matters (OM) make up the major components of marine aerosols, and the chemical  
42 nature determines the hygroscopicity, ice nucleation, and climate impacts of marine aerosols (Huang et al., 2022; Zhao et al.,  
43 2021). Marine organic aerosols (MOA) have attracted attention due to their effects on CCN formation over the remote ocean  
44 (Zhao et al., 2021). Limited understanding on the formation, flux and composition of MOA results in the estimation  
45 uncertainty of climate regulation by marine aerosols (Brooks and Thornton, 2018a; Quinn and Bates, 2011; Quinn et al.,  
46 2015b).

47 Organics are a major fraction in marine aerosols, contributing 3%–90% of submicron aerosol mass (Huang et al., 2018;  
48 O'dowd et al., 2004; O'dowd et al., 2008; Shank et al., 2012). MOA could be primarily released from the ocean surface or  
49 secondarily formed via the oxidation and gas-to-particle conversion of volatile organic compounds (VOCs), including  
50 dimethyl sulfide (DMS), isoprene, etc., in the marine boundary layer (Fu et al., 2011; Trueblood et al., 2019). Ocean surface  
51 is one of the largest active reservoirs of organic carbon on Earth (~18%), resulting from phytoplankton, algal as well as the  
52 related senescence and lysis (Hedges, 1992; Quinn and Bates, 2011). Wave breaking and bubble bursting at the ocean  
53 surface would inject quantities of organic-enriched sea spray aerosols (SSA) into marine atmospheres (Hu et al., 2024;  
54 Quinn et al., 2014). Organic matters are predominant in the fine or submicron SSA, which are usually dominated by water-  
55 insoluble organic carbon (WIOC) (Cavalli, 2004b; Cravigan et al., 2020; Miyazaki et al., 2020). However, the majority of  
56 the water-soluble organic carbon (WSOC) in MOA is contributed by secondary processes via the VOC oxidation or aged  
57 organic aerosols (Schmitt-Kopplin et al., 2012; Trueblood et al., 2019).

58 A recent modeling study suggested that regional emission rates of MOA are largely related to the spatial distribution of  
59 ocean biological productivity (Zhao et al., 2021). During phytoplankton blooms, the organic content elevated to as high as  
60 63% of submicron aerosols, compared to a proportion of 15% during the low biological activity periods (O'dowd et al.,  
61 2004). Seawater chlorophyll-a (*Chl-a*) or its combination with wind speed and aerosol size has been used to parameterize  
62 the organic fraction in SSA (Gantt et al., 2012; Gantt et al., 2011). However, the abundance of various organics in SSA  
63 remains highly uncertain and is a current challenge to understand their role in cloud formation (Albert et al., 2012; Brooks  
64 and Thornton, 2018a).

65 Observation-based parameterization of primary and secondary MOA is urgently needed to constrain the modeling  
66 results (Brooks and Thornton, 2018b; Quinn et al., 2015a). In this work, two shipboard observations of atmospheric aerosols  
67 were conducted from the temperate to the tropical regions over the West Pacific Ocean (WPO) during spring and summer.  
68 Chemical compositions of marine aerosols, including organic carbon and inorganic ions, and seawater parameters were  
69 simultaneously obtained during the cruises. We derived a parameterization to estimate the primarily emitted organic aerosols  
70 in the SSA from wave breaking and bubble bursting, and separated the primary and secondary MOA based on the  
71 observation results. The derived formulation of primary MOA was validated by the measured water-insoluble organics and  
72 protein-like organic matter in marine aerosols, which are primarily generated by sea spray. We further investigated the  
73 spatial distribution, fluorescence characteristics of MOA, and the driving factors of MOA formation over the WPO. Our  
74 results provide an easy observation-based approach to divide the primary and secondary MOA based on the aerosol  
75 components and seawater *Chl-a*, as well as an observation-based parameterization of the primary MOA for further  
76 improving the parameterization of sea spray organic aerosols in large-scale models.

## 77 2 Materials and Methods

### 78 2.1 Cruises and sample collection

79 Two shipboard cruise observations were conducted over the West Pacific Ocean (Fig. 1). Cruise I was conducted in  
80 spring during 19 Feb.–9 April, 2022 on the R/V *KeXue* research vessel, and Cruise II was conducted in summer during 19  
81 June–30 July, 2022 onboard of the R/V *Dongfanghong 3* research vessel. High-volume particle samplers (Qingdao Genstar  
82 Electronic Technology, China) were placed on the upper deck of the ship to collect the total suspended particles (TSP) and  
83 PM<sub>2.5</sub> (particles with a diameter of <2.5  $\mu\text{m}$ ) samples in marine atmospheres. To avoid the contamination of ship exhausts,  
84 the aerosol samplers were placed upwind on the foredeck of the ship. The quartz fiber filters were pre-baked at 500°C for 6 h  
85 before sample collection. The field blank aerosol sample was collected during each cruise.

86 Surface seawater samples were collected by a CTD (conductivity-temperature-depth) assembly (Seabird911). The  
87 concentration of the in-situ seawater *Chl-a* was measured using a fluorescence spectrophotometer (F-4700, Hitachi, Japan)  
88 (Wang et al., 2023a). Surface *Chl-a* concentrations were also obtained based on the satellite-derived data (Siemer et al., 2021;  
89 Tuchen et al., 2023). The satellite-derived *Chl-a* data were provided by Copernicus Marine Environmental Monitoring  
90 Service (CMEMS) with a spatial resolution of 4 km and a monthly temporal resolution (<https://marine.copernicus.eu/>). Here,  
91 we utilized the satellite-derived *Chl-a* data during March and June 2022 to support our conclusion. The concentration of  
92 soluble organic carbon in the seawater was measured by a total organic carbon (TOC) analyzer (TOC-L, Shimadzu, Japan).  
93 Air temperature and wind speed were monitored by the shipborne meteorological station. Surface net solar radiation (SSR)  
94 data were obtained from the hourly data of the ECMWF Reanalysis v5 (ERA5) product (Hersbach et al., 2020), with a  
95 spatial resolution of 0.25°. The 24-hr backward trajectories of air masses (Fig. S1) originating at 500 m above the ground  
96 level were calculated along the observation cruises every 24 hr using the HYSPLIT model (Version 5.2.1, NOAA).

98 **2.2 Aerosol chemical composition analysis**

99 An aliquot of the filter sample was extracted by Milli-Q water ( $>18.2 \text{ M}\Omega\cdot\text{cm}$ ) in ultrasonication, and filtered through  
100  $0.22 \mu\text{m}$  PTFE filters. The extracted solutions were analyzed by ion chromatograph systems (ICS-Aquion and ICS-2100  
101 DIONEX) to obtain the concentrations of water-soluble inorganic ions ( $\text{Na}^+$ ,  $\text{NH}_4^+$ ,  $\text{K}^+$ ,  $\text{Mg}^{2+}$ ,  $\text{Ca}^{2+}$ ,  $\text{Cl}^-$ ,  $\text{NO}_3^-$  and  $\text{SO}_4^{2-}$ ) and  
102 methanesulfonic acid (MSA). The WSOC in the aerosol samples was measured by the TOC analyzer (TOC-L, Shimadzu,  
103 Japan). Organic carbon (OC) and elemental carbon (EC) were analyzed using a Sunset Laboratory thermal/optical carbon  
104 analyzer. Concentration of the water-insoluble organic carbon (WIOC) was calculated by the difference between OC and  
105 WSOC concentrations in each sample. The mass concentration of organic aerosols was calculated by multiplying OC by a  
106 conversion factor 1.6 (Wang et al., 2023b). The OM/OC conversion factor (1.6) was selected based on previous observation  
107 results of marine organic aerosols. Over the North Atlantic, an OM/OC mass ratio of 1.8 was adopted for WSOC based on  
108 the speciation of WSOC performed on the samples, and a conversion factor of 1.2 was applied for WIOC (Cavalli, 2004a).  
109 An average OM/OC ratio of 1.75 was observed in the submicron organic aerosol samples over the Atlantic Ocean (Huang et  
110 al., 2018). A higher proportion of water-soluble secondary organic aerosols (SOA), with higher OM/OC ratios than primary  
111 MOA, was observed in Huang et al. (2018) than in this study. Here, the proportions of WIOC are comparable to (summer  
112 cruise) or higher than (spring cruise) those of WSOC, and thus an OM/OC ratio of 1.6 was selected here. The mass  
113 concentrations of  $\text{PM}_{2.5}$  or TSP were obtained by summing the measured OM, EC, and water-soluble ions in each aerosol  
114 sample. The aerosol samples with  $\text{EC} > 0.2 \mu\text{gC m}^{-3}$  might be influenced by the ship exhausts (Lawler et al., 2020), which  
115 thus were excluded in our discussion. A total of 14 sets of aerosol samples during Cruise I and 17 sets of samples during  
116 Cruise II would be used for further discussion in this work.

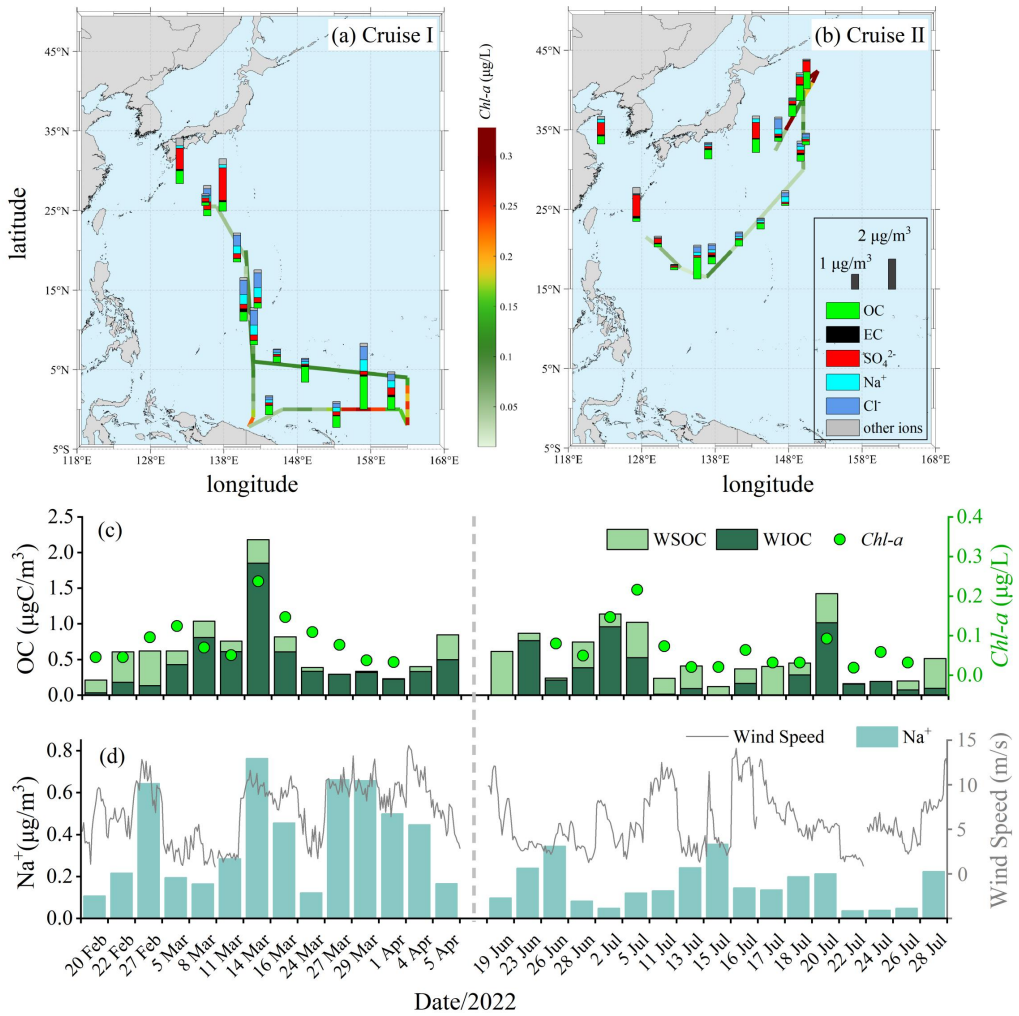
117 **2.3 Fluorescence spectra analysis**

118 Filter aerosol samples were extracted by methanol and filtered through a  $0.22 \mu\text{m}$  PTFE syringe filter. The methanol-  
119 extracted solutions were measured by a fluorescence spectrometer (F98, Lengguang Technology, China) to obtain the  
120 excitation (Ex) and emission (Em) spectra of MOA. Excitation–emission spectra were scanned within 200–600 nm using a 1  
121 cm optical path length. Pre-processing of the fluorescence spectra data included instrument correction, inner filter correction,  
122 Raman and scattering removal, and blank subtraction, which was conducted according to Stedmon and Bro (2008) and  
123 Murphy et al. (2013). Fluorescent components in MOA were identified by excitation-emission matrix-parallel factor (EEM-  
124 PARAFAC) analysis (Murphy et al., 2013; Stedmon and Bro, 2008). The fluorescence intensity was reported using the unit  
125 of  $\text{RU L}^{-1} \text{ m}^{-3}$  after considering the extracted solution volume and air volume of each sample (Fu et al., 2015).

126 **3 Results and Discussion**127 **3.1 Overview of marine organic aerosols during the cruises**

128 The concentrations of the water-soluble ions and carbonaceous aerosols in the fine particles (PM<sub>2.5</sub>) along the cruises  
129 are presented in Fig. 1. The average OC concentration in PM<sub>2.5</sub> was 0.67  $\mu\text{gC m}^{-3}$  (0.21–2.18  $\mu\text{gC m}^{-3}$ ) during the spring  
130 observation and 0.54  $\mu\text{gC m}^{-3}$  (0.12–1.42  $\mu\text{gC m}^{-3}$ ) during the summer observation. The EC concentrations were 0.066  $\pm$   
131 0.056  $\mu\text{gC m}^{-3}$  and 0.055  $\pm$  0.052  $\mu\text{gC m}^{-3}$  during the spring and the summer observations, much lower than those observed  
132 over coastal areas typically influenced by continental outflows (Sahu et al., 2009; Zhang et al., 2025). The observed OC  
133 concentrations during our cruises were comparable to previous studies over the North Pacific Ocean (0.5–0.7  $\mu\text{gC m}^{-3}$ ), and  
134 lower than those observed at an island in the West Pacific Ocean (1.7  $\pm$  1.0  $\mu\text{gC m}^{-3}$ ) (Hoque et al., 2015; Hoque et al., 2017;  
135 Kunwar and Kawamura, 2014). Organic matters were the dominant components in the fine particles, which respectively  
136 contributed 18%–75% (40% on average) and 13%–74% (48% on average) of the PM<sub>2.5</sub> mass in spring and summer. This is  
137 consistent with previous findings that the organic fractions were dominant in the submicron marine aerosols (Facchini et al.,  
138 2008; O'dowd et al., 2004). Film drops could efficiently transfer hydrophobic organic compounds enriched in the air–water  
139 interface into the submicron aerosols, which explained the size-selective enrichment of organics in marine aerosols (Cochran  
140 et al., 2016b; Prather et al., 2013; Quinn et al., 2015a; Wang et al., 2017). The mass concentrations of PM<sub>2.5</sub> were calculated  
141 by summing the measured OM, EC, and water-soluble ions. Metal elements were not measured in this study, which  
142 contributed <3.5% of the marine aerosol mass concentration over the East China Sea (Hsu et al., 2010). Without considering  
143 the metal elements, we may overestimate the organic proportion in marine aerosols. During the sampling, positive artifacts  
144 of OC may exist due to the absorption of gaseous organic vapor on the filters, and negative artifacts may exist due to the  
145 evaporation of volatile organic compounds (Huebert and Charlson, 2000). The OC concentration was measured using  
146 thermal-optical analysis. Quantification uncertainty may be introduced due to the formation of pyrolyzed OC, which  
147 complicates the accurate determination of the OC/EC split point (Cao et al., 2025; Chow et al., 2004).

148 Taking the spring observation as an example, the OC mass in most PM<sub>2.5</sub> samples was roughly equal to that in the  
149 corresponding TSP samples (Fig. S2), which were simultaneously collected using two aerosol samplers during the cruise.  
150 The campaign-averaged OC concentrations were comparable in the PM<sub>2.5</sub> (0.67  $\mu\text{gC m}^{-3}$ ) and the TSP (0.69  $\mu\text{gC m}^{-3}$ )  
151 samples. Thus, our further discussion on marine organic aerosols would focus on the results obtained from the PM<sub>2.5</sub> samples.



152  
153  
154  
155  
156  
157

**Figure 1** Spatial distributions of water-soluble ions and carbonaceous aerosols (organic carbon, OC, and elemental carbon, EC) in the PM<sub>2.5</sub> samples during (a) Cruise I conducted during spring, and (b) Cruise II conducted during summer. Time series of (c) the water-soluble OC (WSOC), water-insoluble OC (WIOC), and Chl-*a*, and (d) Na<sup>+</sup> concentration in aerosol samples and the wind speed during the cruises. In panels (a) and (b), the ship route is colored by the concentration of seawater Chl-*a*. Other ions include NO<sub>3</sub><sup>-</sup>, NH<sub>4</sub><sup>+</sup>, K<sup>+</sup>, Mg<sup>2+</sup> and Ca<sup>2+</sup>.

158 The abundance of MOA displayed similar spatial distribution (Fig. 1) and strong or medium correlations with the sea  
159 surface Chl-*a* concentration (Cruise I:  $r = 0.81$ ,  $p < 0.01$ ; Cruise II:  $r = 0.67$ ,  $p < 0.01$ ), an indicator of the marine biological  
160 activity (Brooks and Thornton, 2018a; Miyazaki et al., 2020). During the biologically active periods, the sea surface layer  
161 was enriched in organics, which would be readily transferred into sea spray aerosols through wave breaking and bubble-  
162 bursting processes (Cochran et al., 2016a; Cochran et al., 2017; Crocker et al., 2022; Wang et al., 2015). The correlation  
163 coefficients between OC and EC were lower (Cruise I:  $r=0.48$ ; Cruise II:  $r = 0.17$ ) than those between OC and seawater Chl-  
164 *a*, suggesting that the potential impacts of transported anthropogenic pollutants were limited during the cruises. The air

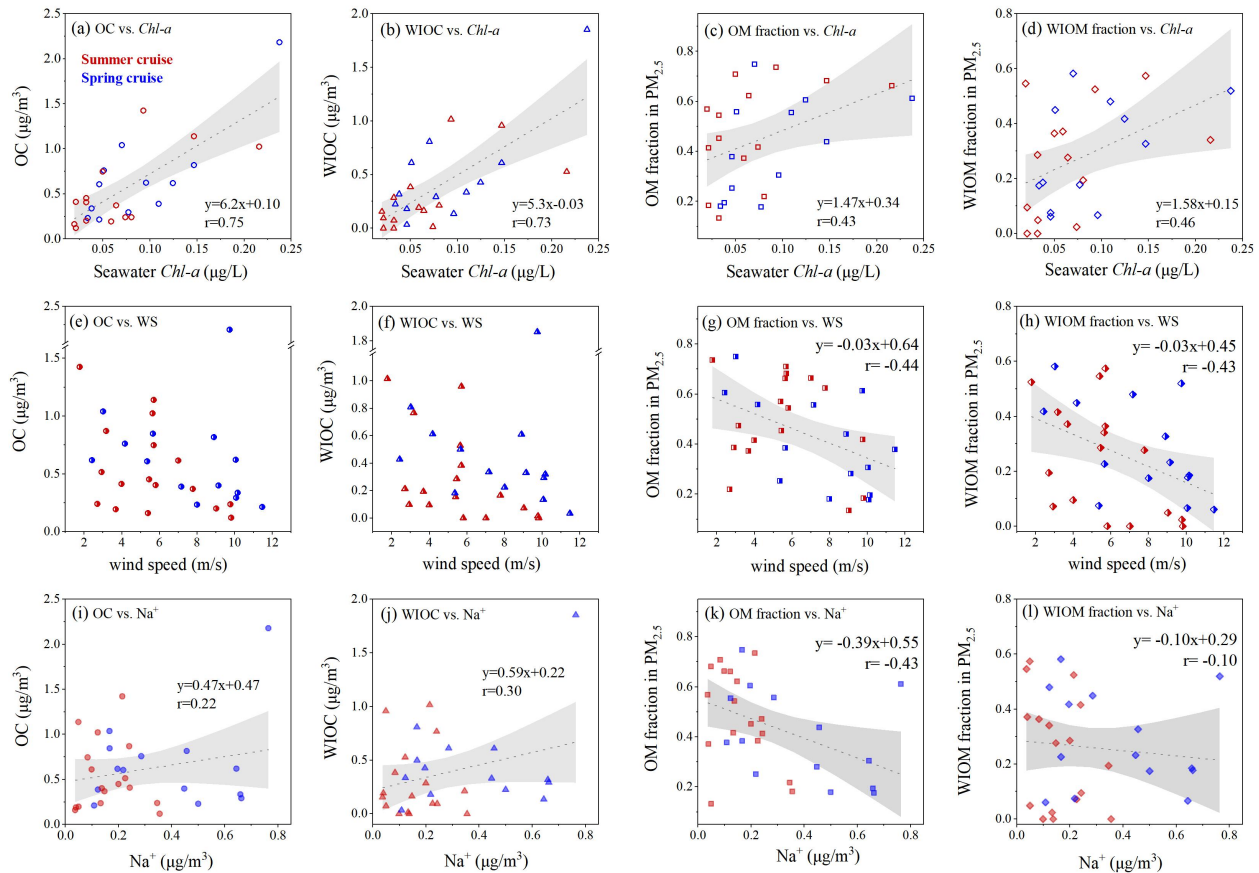
165 masses were mainly transported from open oceanic regions, and thus the impacts of terrestrial outflows were limited during  
166 the cruises (Fig. S1). The OC concentration levels in marine aerosols were higher during the spring cruise than during the  
167 summer cruise (Fig. 1c). This was due to the relatively higher phytoplankton activities along the cruise in spring, indicated  
168 by the higher seawater *Chl-a* in spring ( $0.09 \pm 0.06 \mu\text{g L}^{-1}$ ) than in summer ( $0.07 \pm 0.05 \mu\text{g L}^{-1}$ ). However, the difference was  
169 not significant, with a *P* value of 0.33. The highest OC concentration occurred on 14 March during the spring cruise, when  
170 the highest seawater *Chl-a* ( $0.24 \mu\text{g L}^{-1}$ ) was observed (Fig. 1). For the samples collected near the equator, the MOA or  
171 biogenic VOC precursors could also be transported from coastal oceanic regions of Papua New Guinea and Indonesia with  
172 higher marine biological activity and higher isoprene emission fluxes (Cui et al., 2023; Zhang and Gu, 2022). This could be  
173 an additional reason for the higher OC level during the spring cruise and the highest OC concentration observed on 14 March.  
174

175 The observed concentrations of WSOC and WIOC over the open Pacific Ocean were lower than those observed in the  
176 atmosphere under severe influence of continental outflows (Sahu et al., 2009; Zhang et al., 2025). Marine organic aerosols  
177 were dominated by the water-insoluble fractions, with the WIOC/OC mass ratios of  $70 \pm 27\%$  in spring and  $48 \pm 35\%$  in  
178 summer (Fig. 1). The proportion of water-soluble organics in MOA over the WPO was lower than that observed over the  
179 East Asian marginal seas in autumn (75%), during which severe impacts of continental anthropogenic pollutants were  
180 observed (Zhang et al., 2025). The observed WIOC concentrations showed stronger correlations with the seawater *Chl-a* ( $r =$   
181  $0.79$ ,  $p < 0.01$  in spring and  $r = 0.63$ ,  $p < 0.05$  in summer) than the correlations between WSOC and *Chl-a* ( $r = 0.32$  in spring  
182 and  $r = 0.42$  in summer). This indicated the closer linkage of marine biological-related organics with the WIOC than with the  
183 WSOC in marine aerosols. Marine phytoplankton could produce gel-like aggregates and contribute to extracellular polymer  
184 particles, water-insoluble polysaccharide-containing transparent exopolymer, and protein-containing organics, etc. in  
185 seawater (Aller et al., 2017; Lawler et al., 2020). These organic substances could be enriched in the surface seawater and  
186 then transferred into the atmospheric aerosols within the marine boundary layer. Previous studies suggested that seawater  
187 organics injected into aerosol particles through wave breaking or bubble bursting tend to be more hydrophobic and water  
188 insoluble (Cavalli, 2004b; Facchini et al., 2008; Miyazaki et al., 2010; O'dowd et al., 2004). Water-soluble organics in  
189 marine aerosols are usually related to the aged organic aerosols through long-range transportation or the SOA formed via the  
190 oxidation of marine reactive organic gases (Boreddy et al., 2018; De Jonge et al., 2024; Miyazaki et al., 2010). Reactive  
191 gaseous precursors of organic aerosols are widely observed over different oceanic regions (Tripathi et al., 2024; Tripathi et  
192 al., 2020; Wang et al., 2023a), which contribute to the SOA formation in the marine boundary layer.

### 192 3.2 Correlations of MOA with other parameters

193 The similar variation trends and good correlations between WIOC in marine aerosols and seawater *Chl-a* (Fig. 1, 2)  
194 suggested the origins of MOA from seawater through ocean bubble bursting or wave breaking. Seawater *Chl-a* is a widely  
195 used oceanic parameter to indicate the marine biological activity or the enrichment of organics in marine aerosols (O'dowd et  
196 al., 2004; O'dowd et al., 2008; Rinaldi et al., 2013; Spracklen et al., 2008), which has been employed to predict the organic  
197 fraction in marine aerosols. Over the West Pacific Ocean, we observed better correlations between OC or WIOC

198 concentrations and *Chl-a* than those between organic or water-insoluble organic mass fractions and *Chl-a* (Fig. 2a–2d).  
 199 Some studies reported poor correlations between seawater *Chl-a* and the organic fraction in SSA, and proposed that the  
 200 organic enrichment is also controlled by physical processes, especially the wind-driven sea spray production processes (De  
 201 Leeuw et al., 2011; Lewis and Schwartz, 2004; Salter et al., 2014). Seawater *Chl-a* concentration is one of the most  
 202 important factors driving the variation of organic fraction in the SSA, and they display good correlations when the wind  
 203 speed does not vary a lot. However, wind speed should be combined with surface *Chl-a* to predict the organic fraction in  
 204 SSA if the wind speed varies obviously during the observation or simulation periods (Gantt et al., 2011; Grythe et al., 2014).  
 205 This is due to the influence of wind on the coverage of sea surface microlayer (SML) in the sea surface, which is enriched in  
 206 organic compounds. For a given chemical composition of seawater, the largest coverage of sea surface by SML and a higher  
 207 organic fraction in SSA are expected during calm winds. However, the SML would be destructed by mixing into the  
 208 underlying seawater and the organic fraction in SSA decreased when surface wind exceeded 8 m s<sup>-1</sup> (Gantt et al., 2011).  
 209 Thus, researchers usually combine wind speed with surface *Chl-a* to predict the organic fraction in SSA (Gantt et al., 2011;  
 210 Grythe et al., 2014).



212 **Figure 2** The scatter plots of OC, WIOC concentrations or fractions in marine aerosols as a function of (a-d) surface  
213 seawater *Chl-a*, (e-h) wind speed (WS) and (i-l)  $[\text{Na}^+]$  in  $\text{PM}_{2.5}$  samples during the two cruises. The data points during the  
214 springtime Cruise I and the summertime Cruise II are in blue and red, respectively. The regression line in each panel  
215 represents the correlation between the two parameters during the two cruises with a 95% confidence band.

216 During our cruises over the WPO, the concentrations of OC or WIOC in  $\text{PM}_{2.5}$  showed a decreasing trend with the  
217 increase of wind speed (Fig. 2e, 2f). The organic fraction in marine aerosols displayed a negative correlation with the wind  
218 speed (Fig. 2g, 2h). The organic-enriched SML in the sea surface would be destructed under high wind speed conditions,  
219 which results in a decrease of organic substances transported into the SSA (Gantt et al., 2011). The concentration or  
220 proportion of  $\text{Na}^+$  in the marine aerosols showed positive correlations with the wind speed during the observations (Fig. S3).  
221 Atmospheric SSA are primarily released as a mixture of inorganic sea salt and organic matters from the ocean surface. We  
222 observed weak positive correlations between OC or WIOC and  $\text{Na}^+$  concentrations (Fig. 2i, 2j). We proposed that, for the  
223 filter-based observation or the samplings with a similar time resolution,  $\text{Na}^+$  in fine particles could be used as a better  
224 indicator of the overall organic production levels than the wind speed in marine atmospheres. The  $[\text{Na}^+]$  represents the bulk  
225 sea salt abundance generated by wave breaking and bubble bursting, and reflects the overall effects of wind speeds and other  
226 meteorological conditions on SSA production during the period of filter sample collection. Russell et al. (2010) found strong  
227 correlations between ocean-derived submicron organic aerosols and  $\text{Na}^+$  concentrations (Russell et al., 2010). It should be  
228 noted that dust storms also transport  $\text{Na}^+$  to marine atmospheres, especially over the marginal seas (Zhang et al., 2025).  
229 When using  $\text{Na}^+$  in marine aerosols as the indicator of SSA production, the  $\text{Na}^+$  contributed by transported dust storms  
230 should be excluded, especially during dust episodes. For the collected TSP samples, the OC concentrations did not display  
231 an obvious correlation with the seawater *Chl-a* (Fig. S4). This is because the dominant production processes of OC and sea  
232 salts are different. Organic matters in marine aerosols are enriched in the submicron SSA, which is mainly formed by film  
233 drops from bursting bubble-cap films (Wang et al., 2017). In contrast, the majority of the sea salt mass exist in larger  
234 supermicron or coarse-mode particles generated by jet drops from the base of bursting bubbles (Wang et al., 2017).

### 235 **3.3 Estimation of primary and secondary MOA**

236 Based on the correlation analysis of the observed parameters, we proposed a parameterization scheme to separate the  
237 marine primarily-emitted OC (MPOC) in the SSA generated through wave breaking or bubble bursting processes and the  
238 secondarily formed organic carbon (MSOC) in the marine aerosols over WPO. For a given marine environment condition (a  
239 given *Chl-a*, wind speed, sea surface temperature (SST), etc.), the abundance of MPOC should be constant (Gantt et al.,  
240 2011). Seawater *Chl-a* concentration is the most important factors driving the variation of organic fraction in the SSA, and  
241 has been widely used to estimate the organic fraction in SSA (Gantt et al., 2011; Vignati et al., 2010). For given chemical  
242 composition of seawater, the largest organic fraction in SSA is expected during calm winds. An increase in wind speed  
243 above 3–4  $\text{m s}^{-1}$  will cause a rapid decrease of organic fraction due to the destructing of the SML coverage, and the lowest  
244 organic fraction is expected for wind exceeded 8  $\text{m s}^{-1}$  (Gantt et al., 2011). Seawater temperature is related to the production

efficiency and the number concentrations of SSA (Christiansen et al., 2019). In other words, it is a consistent relation between the MPOC and the sea surface *Chl-a* when the marine environment conditions remain stable. Sea surface *Chl-a* and wind speed have been utilized to parameterize the MPOC in global models (Gantt et al., 2012). Based on the shipboard observations in the present study, the mass ratio of the bulk OC (unit:  $\mu\text{g C m}^{-3}$ ) versus seawater *Chl-a* (unit:  $\mu\text{g L}^{-1}$ ) ranged from  $3.0 \times 10^{-3}$  to  $1.9 \times 10^{-2}$ . The increased ratios or fitting line slope of OC versus *Chl-a* relevant to the lowest ones were attributed to the favorable marine conditions for the SSA generation, and the elevated contribution of SOA (e.g., methanesulfonic acid from DMS oxidation, isoprene SOA contributed by phytoplankton emission) (Barnes et al., 2006; De Jonge et al., 2024; Gupta et al., 2025; Ma et al., 2024; Wang et al., 2023b). The MSOC here includes the organic aerosols formed via gas-to-particle conversion of gaseous precursors and oxidation/aging processes of primary OC. The idea is conceptually similar to the classic OC/EC ratio method (Lim and Turpin, 2002; Turpin and Huntzicker, 1995), which uses EC as the tracer and has been widely used to estimate the primary and secondary OC in the continental atmospheres. Here we explored a formulation to estimate the MPOC and MSOC based on the observed OC and  $\text{Na}^+$  in marine aerosols and the seawater *Chl-a*:

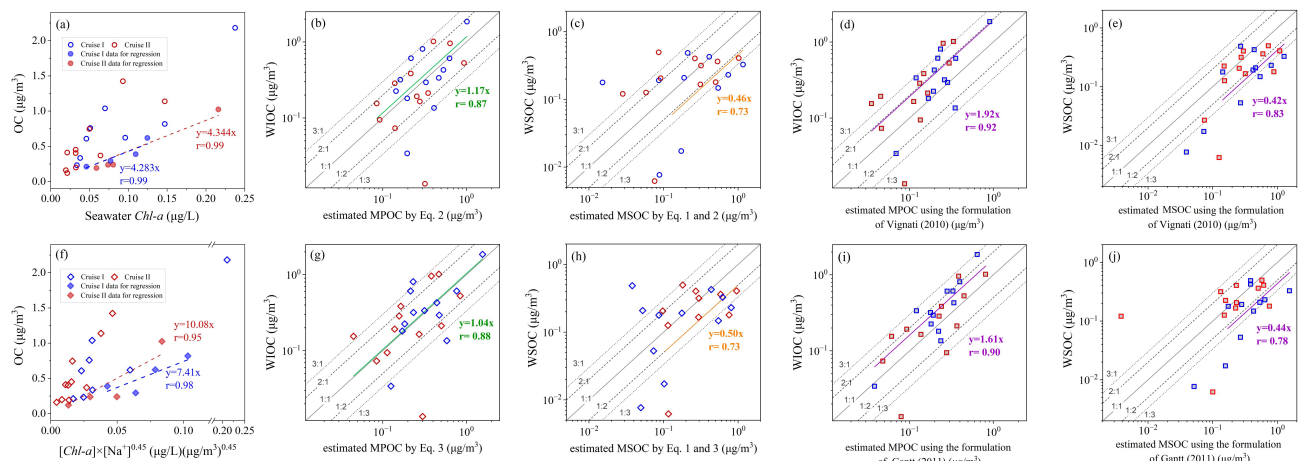
$$[\text{OC}] = [\text{MPOC}] + [\text{MSOC}] \quad \text{Eq. 1}$$

$$[\text{MPOC}] = [\text{Chl} - a] \times \left( \frac{[\text{OC}]}{[\text{Chl}-a]} \right)_{\text{SSA}} \quad \text{Eq. 2}$$

$$[\text{MPOC}] = ([\text{Chl} - a] \times [\text{Na}^+]^p) \times \left( \frac{[\text{OC}]}{[\text{Chl}-a] \times [\text{Na}^+]^p} \right)_{\text{SSA}} \quad \text{Eq. 3}$$

where the  $[\text{OC}]$  is the total OC concentration in the marine aerosols, and  $[\text{Chl}-a]$  is the concentration of surface seawater *Chl-a*. The  $\left( \frac{[\text{OC}]}{[\text{Chl}-a]} \right)_{\text{SSA}}$  in equation (2) represents the ratio of  $[\text{OC}]$  versus  $[\text{Chl}-a]$  in SSA, and  $\left( \frac{[\text{OC}]}{[\text{Chl}-a] \times [\text{Na}^+]^p} \right)_{\text{SSA}}$  in equation (3) is  $[\text{OC}]$  versus  $([\text{Chl}-a] \times [\text{Na}^+]^p)$  in the primary SSA.

264



265  
266 **Figure 3** The scatter plots of OC in marine aerosols as a function of (a) seawater *Chl-a* and (f)  $([\text{Chl}-a] \times [\text{Na}^+]^{0.45})^{1/0.45}$  during  
267 the two cruises; (b, g) Comparison of WIOC and the estimated MPOC based on the regression in panel (a) and panel (f); (c, (i))

268 h) Comparison of WSOC and the estimated MSOC; (d, i) Comparison of WIOC and the estimated MPOC, and (e, j)  
269 Comparison of WSOC and the estimated MSOC using the formulation of Vignati (2010) and Gantt (2011). The dashed lines  
270 in panels (a, f) are the regression line of [OC] and [Chl-a] or  $([Chl-a] \times [Na^+]^{0.45})$  with 0–30% percentile ratios, indicated by  
271 solid markers, during Cruise I (blue) and Cruise II (red). The regressions line in panels (b–e, g–j) represent the correlation  
272 between WIOC and the estimated MPOC or between WSOC and the estimated MSOC in each panel during the two cruises.

273 Here, Eq. 2 or Eq. 3 is used to estimate the concentrations of MPOC based on the seawater [Chl-a] without or with  
274 considering the simultaneously measured  $Na^+$  concentrations as the input parameters. When  $p=0$ , Eq. 3 is the same  
275 formulation as Eq. 2 without the  $Na^+$  as an input parameter. Based on the correlation analysis, the MOA abundance was  
276 mainly driven by the Chl-a abundance. We used Chl-a as the parameter to predict the concentration of MPOC in Eq. 2. For  
277 the samples with the lowest 30% percentile of [OC]/[Chl-a] ratios, we proposed that the generation of organic aerosols was  
278 dominated by the primary sea spray. The dataset with 0–30% percentile of [OC]/[Chl-a] ratios, indicated by the solid  
279 markers in Fig. 3a, was used to calculate the fitting line of MPOC versus [Chl-a]. This is similar to the classic OC/EC ratio  
280 method (Turpin and Huntzicker, 1995). The OC/EC ratios in POC is usually calculated based on the dataset with the lowest  
281 10%–20% percentile OC/EC ratios observed during the campaign, which is then used to separate the POC and SOC in each  
282 aerosol sample (Lim and Turpin, 2002; Yu et al., 2021). We used the data with the lowest 30% percentile of [OC]/[Chl-a]  
283 ratios, considering the number of data points to calculate the fitting curve of MPOC versus [Chl-a]. With more data points,  
284 the data with the lowest 10%–20% percentile [OC]/[Chl-a] ratios could be used to estimate the [MPOC]/[Chl-a] ratios, and  
285 the estimated MPOC abundance may be a little higher than the results using the lowest 30% percentile data. The ratios of  
286 [MPOC]/[Chl-a] were 4.28 during cruise I and 4.34 during cruise II (slopes of the fitting lines in Fig. 3a), which were then  
287 used to estimate the MPOC during each cruise. The performance of MPOC parameterization was evaluated by comparing the  
288 estimated concentrations of MPOC with the WIOC concentrations, which is generally considered as a proxy for MPOC (Fig.  
289 3b). The average mass ratio of WIOC versus MPOC was 1.17 ( $r=0.87$ ), and 69% of the data points fall within the 1:2 and 2:1  
290 line (Fig. 3b). The shipboard observations suggested that the OC concentrations primarily generated by sea spray over the  
291 WPO could be approximately estimated by  $4.3 \times [Chl-a]$  when other related parameters were absent.

292 A combined parameterization scheme of multiplying seawater [Chl-a] by  $[Na^+]^p$  was also used to predict the  
293 concentration of MPOC (Eq. 3). A weak correlation between OC and  $Na^+$  was observed here (Fig. 2i, 2j), and we thus  
294 combined  $[Na^+]$  as the input parameter to reflect the variation of the bulk sea spray aerosol abundance. In the scatter plot of  
295 OC and  $([Chl-a] \times [Na^+]^p)$ , taking  $p=0.45$  as an example in Fig. 3f, we proposed that the generation of organic matters were  
296 dominated by the primary sea spray in the samples with the lowest 30% percentile of  $[OC]/([Chl-a] \times [Na^+]^p)$  ratios. The  
297 dataset with 0–30% percentile of  $[OC]/([Chl-a] \times [Na^+]^{0.45})$  ratios, indicated by the solid markers in Fig. 3f, was used to  
298 calculate the fitting line of MPOC versus  $[OC]/([Chl-a] \times [Na^+]^{0.45})$ . The fitting line was then employed to estimate the  
299 MPOC in other marine aerosol samples based on the seawater Chl-a and the aerosol  $Na^+$  concentrations. In each sample, the  
300 increased OC concentration relevant to the MPOC fitting line is attributed to the additional contribution by MSOC.

301 We compared the estimated MPOC and the measured WIOC to evaluate the performance of the MPOC  
302 parameterization and determine the  $p$  value in equation 3. Both the correlation coefficients ( $r$ ) and the slopes of the fitting

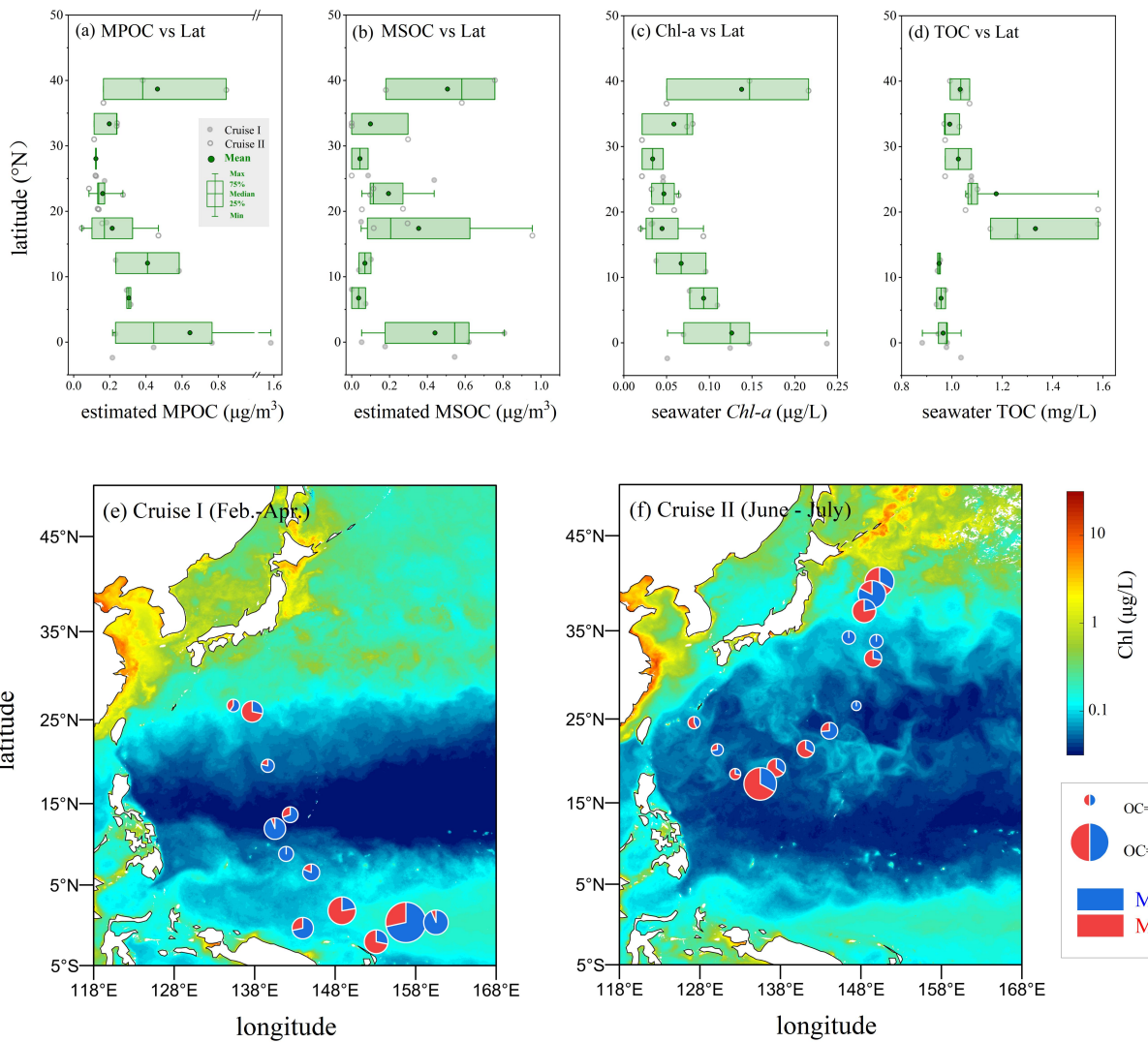
303 line between WIOC and estimated MPOC are used to evaluate the performance of different MPOC parameterization  
 304 approaches. It means that the estimated MPOC shows a similar variation trend to WIOC if with a  $r$  value closer to 1, and a  
 305 good comparison with the WIOC mass concentrations if with a fitting line slope closer to 1. We tested the performance of  
 306 the MPOC formulation when changing the  $p$  value from 0–1, with an interval of 0.05. The variations of the fitting line slopes  
 307 and correlation coefficients of WIOC and MPOC are shown in Fig. S3. When using a  $p$  value of 0.35–0.65, the estimated  
 308 MPOC matched well with WIOC concentrations, with the fitting line slopes of 1.03–1.05 and the  $r$  values of 0.86–0.88.  
 309 When using  $p=0.45$ , both the fitting line slope (1.036) and  $r$  value (0.88) suggested an overall better performance than using  
 310 other  $p$  values (Fig. S5, 3g). Without the  $[Na^+]$  as an input parameter, the fitting line slope and  $r$  of WIOC and MPOC were  
 311 respectively 1.17 and 0.87 (Fig. 3b), suggesting an underestimation of MPOC. In further analysis, we employed Eq. 3 with  
 312  $p=0.45$  to estimate the MPOC. A total of 58% of the estimated data points fell within the WIOC/MPOC 2:1 and 1:2 lines  
 313 (Fig. 3g), and 73% fell within the 3:1 and 1:3 lines, during the two cruises. The estimated MSOC matched better with the  
 314 WSOC in the marine aerosols when using a combination of  $[Chl-a]$  and  $[Na^+]$  (equations 1 and 3) as the input parameters  
 315 and considering the variation of sea spray aerosols (Fig. 3c, 3h). Based on equations 1 and 3, the estimated MSOC  
 316 concentrations in half of the samples fall within the WSOC/MSOC 3:1 and 1:3 lines, and the fitting line slope (0.50) was  
 317 closer to 1 (Fig. 3h). Using equations 1 and 2, the fitting line slope of WSOC and estimated MSOC was 0.46, and 46% of the  
 318 estimated MSOC concentrations fall within the WSOC/MSOC 3:1 and 1:3 lines (Fig. 3c). It is noted that, based on the  
 319 shipboard in-situ observation, we cannot exclude the potential impacts of gaseous precursors or aged organic aerosols long-  
 320 range transported from terrestrial environments, which were mostly in the MSOC fraction. The organic aerosols transported  
 321 from terrestrial environments were secondary or aged organic aerosols, and tend to be water-soluble organic compounds  
 322 (Boreddy et al., 2018; De Jonge et al., 2024; Miyazaki et al., 2010). Based on the air mass back trajectories (Fig. S1) and the  
 323 weak correlations between OC and EC stated in section 3.1, the impacts of transported continental outflows were limited  
 324 during the cruises.

325 The MPOC was also estimated using the formulations in literatures (Gantt et al., 2011; Vignati et al., 2010) based on  
 326 the observed seawater  $Chl-a$ , OC and  $Na^+$  in aerosols as well as the wind speed observed during the cruises over the WPO  
 327 (Fig. 3d, 3i). Vignati et al (2010) estimated the organic mass fraction in sea spray aerosol (OM<sub>SSA</sub>) using seawater  $[Chl-a]$ :  
 328 
$$\%OM_{SSA} = 43.5 \times [Chl-a](mg\ m^{-3}) + 13.805$$
. Gantt et al (2011) predicted the OM<sub>SSA</sub> using a combination of  $[Chl-a]$  and  
 329 10 m wind speed ( $U_{10}$ ): 
$$OM_{SSA}(Chl - a, U_{10}) = \frac{OM_{SSA}^{max}}{1 + \exp(-2.63[Chl-a] + 0.18U_{10})}$$
, where  $OM_{SSA}^{max}$  is the maximum  $OM_{SSA}$  observed  
 330 during the cruises. The estimated MPOC displayed good correlations with the observed WIOC. However, the abundance of  
 331 MPOC was underestimated approximately by 38%–48% through comparing with the WIOC concentrations (Fig. 3d, 3i).  
 332 The estimated MSOC using the parameterizations from Gantt et al. (2011) or Vignati et al. (2010) showed similar variation  
 333 trends to the WSOC in the collected aerosols samples. The comparison of the estimated MSOC and the WSOC  
 334 concentrations using formulations in literatures (slopes in Fig. 3e, 3j), however, were not as good as those estimated in this  
 335 study (slopes in Fig. 3h). The MPOC source functions in Gantt et al. (2011) and Vignati et al. (2010) were proposed based

336 on the observation over the North Atlantic, which has been widely employed in large-scale models. These parameterizations  
337 perform well to trace the variation trends of MPOC. However, they might lead to an underestimation of the primary MOA  
338 over the West Pacific Ocean. This is mainly due to different seawater compositions, marine environment or atmospheric  
339 meteorological conditions in the North Atlantic and the West Pacific Oceans, which result in different quantitative relations  
340 between seawater *Chl-a* and MPOC in these oceanic regions. What's more, the seawater *Chl-a* was determined using the  
341 spatial average of the satellite-derived *Chl-a* concentrations in Gantt et al. (2011). This could be an additional reason for the  
342 different parameterizations between *Chl-a* and MPOC compared with the results based on the in-suit measured *Chl-a* in this  
343 work. The results highlight different quantitative relations of MPOC with seawater *Chl-a* and other parameters in different  
344 areas, which are needed to be provided through in-situ observations across different oceanic regions and to constrain in  
345 global models.

346 **3.4 Spatial distribution and driving factors of primary and secondary MOA**

347 Based on the validated formulation, concentrations of MPOC and MSOC in the marine aerosols over the WPO are  
348 estimated. Here we employed Eq. 3, with  $p=0.45$ , for the estimation of MPOC. The concentrations and relative contributions  
349 of MPOC and MSOC along the latitude are shown in Fig. 4. The estimated MPOC was respectively  $0.43 \pm 0.40$  and  $0.24 \pm$   
350  $0.21 \mu\text{gC m}^{-3}$ , averagely accounting for  $66\% \pm 27\%$  and  $56\% \pm 30\%$  of the total OC in marine aerosols, during the  
351 springtime Cruise I and the summertime Cruise II. The dominant contribution of MOA by the marine fresh carbon pool was  
352 also observed during the Arctic cruises, during which the MPOC contributed 80% of the carbonaceous fraction based on the  
353 stable carbon isotopic signature (Gu et al., 2023). The estimated MSOC concentrations were comparable in spring ( $0.25 \pm$   
354  $0.28 \mu\text{gC m}^{-3}$ ) and in summer ( $0.27 \pm 0.30 \mu\text{gC m}^{-3}$ ) over the WPO. The SOA fraction among the total organic aerosols was  
355 higher during the summer cruise (44% on average) than during the spring (34% on average).



356

357 **Figure 4** The variations of (a) estimated MPOC, (b) MSOC, (c) seawater *Chl-a* and (d) TOC along the latitude during the  
358 two cruises over the WPO. Spatial distributions of the estimated MPOC and MSOC during (e) the springtime Cruise I, and (f)  
359 the summertime Cruise II. Ocean is coloured by the sea surface *Chl-a* concentrations in March (panel e) and July (panel f),  
360 2022. The marker size in panels (e, f) represents the observed OC concentration in each sample.

361 Both MPOC and MSOC displayed high concentrations over the oceanic regions among 5°S–5°N ( $0.64 \pm 0.56$  and  $0.44$   
362  $\pm 0.32 \mu\text{gC m}^{-3}$ ) and 35°N–40°N ( $0.46 \pm 0.35$  and  $0.51 \pm 0.30 \mu\text{gC m}^{-3}$ ), which were consistent to the spatial distribution of  
363 the sea surface *Chl-a* (Fig. 4). In contrast to the findings over the North Atlantic that plankton had little impact on the  
364 chemical compositions of SSA (e.g., organic mass fraction) (Bates et al., 2020), we observed a positive correlation between  
365 MOA and seawater *Chl-a* and the driving effects of surface *Chl-a* on the abundance of primary MOA over the WPO (Fig. 2,

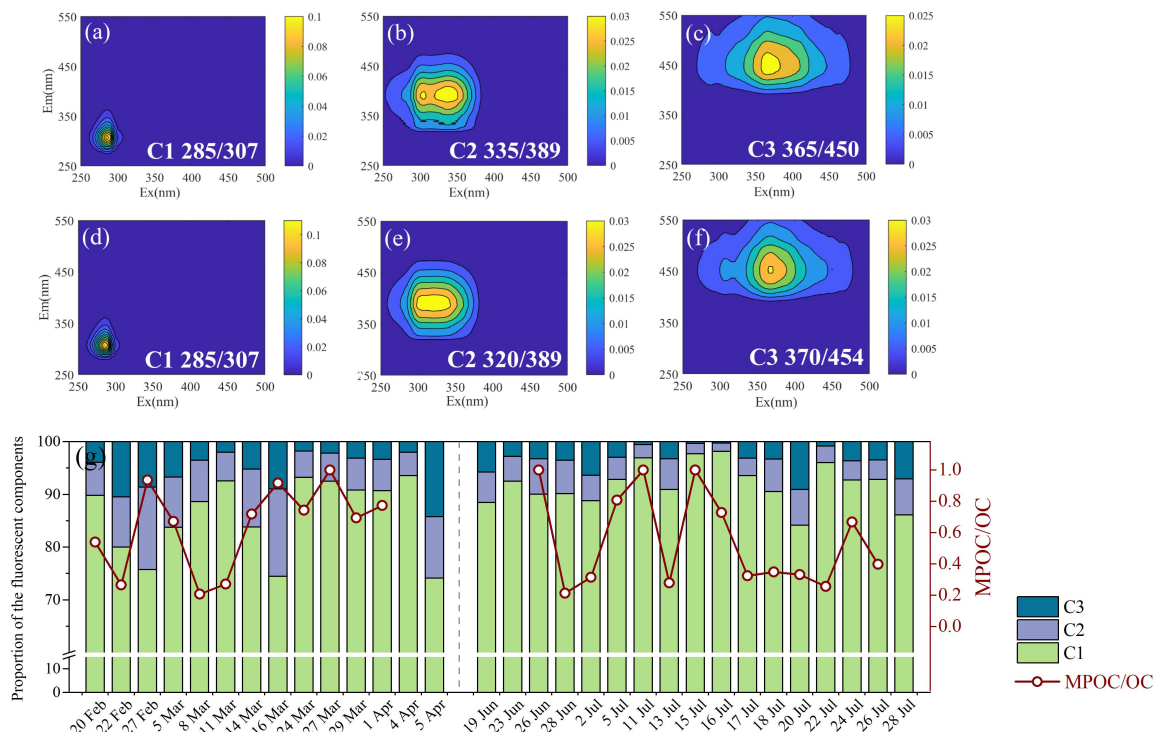
366 4). In addition, the observation areas within 35°N–40°N were the Kuroshio Oyashio Extension (KOE) region, where the  
367 nutrient enrichment driven by upwelling favored the phytoplankton growth and resulted in elevated seawater *Chl-a* levels  
368 (Wang et al., 2023a). The extreme physical disturbance in the KOE further promoted the sea spray-generated organics from  
369 seawater as well as the production of VOCs from phytoplankton. Based on the air mass back trajectories (Fig. S1), the  
370 impacts of transported terrestrial outflows were limited among the observation regions. Marine organic aerosols or biogenic  
371 VOC precursors could also be transported from coastal oceanic regions with higher *Chl-a* levels and higher isoprene  
372 emission fluxes (Cui et al., 2023; Zhang and Gu, 2022), which could be an additional reason for the higher MOA  
373 concentrations within 5°S–5°N and 35°N–40°N.

374 The MSOC also displayed a peak over the areas among 15°N–20°N ( $0.35 \pm 0.41 \mu\text{gC m}^{-3}$ , Fig. 4b), which could be  
375 attributed to the additional contribution by abiotic VOC precursors from the photochemical production in the sea surface  
376 microlayer and their further oxidation in marine boundary layer (Bruggemann et al., 2018). Previous studies suggested that  
377 interfacial photochemical degradation of dissolved organic matters in seawater could be an important source of marine  
378 VOCs (e.g., isoprene) on a global scale (Bruggemann et al., 2018; Cui et al., 2023; Wang et al., 2023a; Yu and Li, 2021). For  
379 remote oceanic regions with high solar radiation but low biological activities, interfacial photochemistry of surface organics  
380 could be a major source of abiotic VOCs in the marine boundary layer (Bruggemann et al., 2018; Cui et al., 2023). Higher  
381 concentration levels of the surface seawater TOC concentrations were observed along the summer cruise within 15°N–20°N  
382 (Fig. 4d). The strong solar radiation during the summertime (19 June- 30 July) Cruise II, as shown in Fig. S6, favored the  
383 photochemical VOC production and the SOA formation in marine atmospheres. During the summer cruise, the estimated  
384 MSOC/OC ratios over the oceanic regions of 15°N–20°N were 65%–72%, and the SOA formation drove the elevation of  
385 MOA concentrations over this area during summer (Fig. 4f).

386 Aerosol samples were collected among 15°N–30°N during both the spring and the summer cruises, which were  
387 compared to elaborate the seasonal difference. The variations of the estimated MPOC and MSOC along the latitude are  
388 shown in Fig. S7, S8. Among the observation region within 15°N–30°N, the average MPOC was comparable in spring ( $0.16 \mu\text{gC m}^{-3}$ ) and summer ( $0.18 \mu\text{gC m}^{-3}$ ), with the average *Chl-a* concentration  $0.042$  and  $0.044 \mu\text{g L}^{-1}$ , respectively. Among the  
389 oceanic regions with similar concentrations of seawater *Chl-a*, the MPOC abundance in marine aerosols was comparable  
390 without seasonal difference. Among 15°N–30°N, the elevation of MPOC concentrations was consistent with the elevated  
391 seawater *Chl-a* concentration without seasonal difference (Fig. S7a). This is consistent with the finding that marine biogenic  
392 activities drive the MPOC production. The average MSOC concentration was  $0.24 \mu\text{gC m}^{-3}$  within 15°N–30°N in summer,  
393 higher than that in spring ( $0.19 \mu\text{gC m}^{-3}$ ). The elevated MSOC was driven by the increase of seawater TOC concentrations  
394 (Fig. S8b). What's more, the stronger solar radiation in summer (Fig. S6) favored the photochemical VOC production in  
395 SML, their further photo-oxidation reactions, and the MSOC formation in the atmosphere.

## 397 3.5 Fluorescence characteristics of MOA

398 The fluorescence spectrum of MOA was analyzed to gain a further understanding on the composition characteristics of  
 399 MOA over the WPO. Based on the EEM PARAFAC analysis, three fluorescent components were identified in marine  
 400 organic aerosols during each cruise observation (Fig. 5, S4). Similar fluorescence components were resolved during the  
 401 Cruise I (Fig. 5a-5c) and Cruise II (Fig. 5d-5f). Each component was named based on the fluorescence characteristics and the  
 402 temporal variation of the fluorescent intensity. Component 1 (C1) shows a peak ( $\text{Ex/Em} = 285/307$  nm) identical to the  
 403 protein-like substances (PRLIS) (Chen et al., 2016b). The PRLIS are enriched in the surface seawater and could be injected  
 404 into SSA via bubble bursting (Miyazaki et al., 2018a; Santander et al., 2021). The similar variations of C1 intensity and  $\text{Na}^+$   
 405 in the marine aerosols, especially during the summer observation (Fig. S9), suggested the origins of PRLIS from marine  
 406 biological materials (Fu et al., 2015; Santander et al., 2022). Thus, C1 was designated as marine PRLIS. Component 2 (C2)  
 407 has a peak  $\text{Ex/Em} = 320-335/389$  nm (Fig. 5), which is related to terrestrial humic-like substances (HULIS) (Chen et al.,  
 408 2016b). Component 3 (C3) displayed the fluorescence characteristics of oxygenated HULIS, with a peak  $\text{Ex/Em} = 365-$   
 409 370/450-455 nm (Fig. 5). The intensities of C2 and C3 showed similar variations to the concentrations of EC and sulfate in  
 410 marine aerosols (Fig. S9), which indicated their sources related to combustion emission and secondary formation (Tang et al.,  
 411 2024). Oxygenated HULIS included the secondarily-formed and aged organic aerosols from both terrestrial and marine  
 412 sources.



413

414 **Figure 5** (a-f) The excitation (Ex) and emission (Em) spectra of the identified fluorescent components: C1: marine protein-  
415 like substances (PRLIS), C2: terrestrial humic-like substances (HULIS), C3: oxygenated HULIS. (g) Time series of the  
416 fluorescent component relative abundances and the MPOC/OC mass ratios in the marine aerosols over the West Pacific  
417 Ocean.

418 The fluorescent components of the MOA were dominated by the PRLIS primarily emitted by the sea spray (C1 shown  
419 in Fig. 5a, 5d), which contributed 74%–94% (86% on average) and 84%–98% (92% on average) of the MOA fluorescent  
420 intensity during Cruise I and Cruise II, respectively (Fig. 5g). It is noted that the proportion of different fluorescent  
421 compounds did not represent their mass contributions, as the fluorescent efficiency of organic compounds was related to their  
422 chemical structures. Organic molecules with substantial conjugation of  $\pi$ -bonds or double bound structures are known to be  
423 especially efficient at emitting fluorescence, particularly when N atoms are present (Chen et al., 2016a; Pöhlker et al., 2012).  
424 Amino acids, vitamins, and humic-like substances have been identified as efficient fluorophores (Graber and Rudich, 2006;  
425 Laskin et al., 2015; Pöhlker et al., 2012). The sea-to-air transfer of phytoplankton-produced protein-containing organics  
426 leads to a significant enhancement of fluorescent compounds in SSA (Aller et al., 2017; Lawler et al., 2020; Miyazaki et al.,  
427 2018b). The PRLIS, or named protein-like organic matter (PLOM), has been identified as a common component in the  
428 oceanic organic matter, and enriched in marine aerosols (Chen et al., 2016b). However, the biogenic SOA (e.g., isoprene  
429 oxidation products abundant in marine atmospheres) molecules, without conjugated double bounds, are weakly fluorescent  
430 or do not display fluorescent properties (Carlton et al., 2009; Laskin et al., 2015). Thus, the WSOC contributed by biogenic  
431 SOA was not included in the detected fluorescent components, and the observed proportions of PRLIS emitted by sea sprays  
432 was higher than those of the WIOC mass contribution in the marine aerosols.

433 During the summertime Cruise II, the fluorescent intensity and the relative contribution of marine-emitted PRLIS (C1)  
434 were higher than those during Cruise I. During the summer cruise, the contribution of the marine PRLIS among the total  
435 fluorescent organic aerosols displayed a similar variation trend to the mass fraction of the estimated MPOC (Fig. 5g). The  
436 variation of the marine PRLIS (C1) intensity was consistent to the seawater *Chl-a* concentration in summer (Fig. S9). This  
437 further indicated the dominant contribution of primary MOA in marine organic aerosols, which could be attributed to the  
438 marine biological materials and injected into the atmosphere through bubble bursting. The marine biological PRLIS could be  
439 related to tryptophan-like or tyrosine-like components as well as the non-nitrogen-containing organic compounds in  
440 atmospheric aerosols (Chen et al., 2016b).

#### 441 **4 Summary**

442 In-situ shipboard observations were conducted to investigate the abundance and composition of MOA over the open  
443 Pacific Ocean. We proposed a formulation to separate and estimate the primary and secondary MOA based on the seawater  
444 *Chl-a* or its combination with  $\text{Na}^+$  in marine aerosols. Based on the validated formulation, the estimated MPOC accounted  
445 for 56%–66% of the total OC in the marine aerosol samples, which were mostly related to the protein-like substances from  
446 seawater biological materials. Both the MPOC and the MSOC displayed peak concentrations among 5°S–5°N and 35°N–

447 40°N over the West Pacific Ocean. The spatial distribution of MOA along the latitude was driven by the marine biological  
448 activities, indicated by the seawater *Chl-a*. For the secondary MOA, high concentrations were also observed over the region  
449 of 15°N–20°N, which was attributed to an additional contribution by the secondary oxidation of VOCs generated from the  
450 photochemical production of seawater organics.

451 This study provides a parameterization to estimate the primary and secondary MOA based on the shipboard observation  
452 evidence, and highlights the marine biogenically driven MOA formation over the North Pacific Ocean. For the observation  
453 studies, our results provide an easy approach to separate the primary and secondary MOA with different chemical natures,  
454 based on the seawater *Chl-a* and aerosol components (OC, Na<sup>+</sup>). The approach is not dependent on the organic tracers,  
455 usually obtained through complex analysis procedures, or limited to the time resolution of sample collection. In previous  
456 studies, fractions of organics in marine aerosols have been estimated based on an empirical relationship of satellite-derived  
457 oceanic *Chl-a*, or a combination with wind speed and aerosol size distribution (Gantt et al., 2012; Li et al., 2024; Wang et al.,  
458 2024). Here, we gain the quantitative relations of primarily-generated marine organic aerosols with sea salts and *Chl-a* based  
459 on measurement results of the marine aerosols and seawater. For the modelling studies, the sea salt flux has been better  
460 estimated than that of marine organic aerosols in global models (Gantt and Meskhidze, 2013). The MPOC formulation here  
461 would help to improve the parameterization of MOA in models and better understand the climate effects of marine aerosols  
462 on a global scale.

463  
464  
465  
466  
467

## 468 **Data availability**

469 The data is available via <https://zenodo.org/records/16831992> (Wang, 2025)

## 470 **Author contributions**

471 Y.W. designed the research. Y.Y., Y.Z., S.L., H.Z., and S.Y. conducted the measurements. Y.Y. and Y.W. analyzed the data.  
472 Y.W., Y.Y. and W.X. wrote the manuscript with contributions from all authors.

## 473 **Acknowledgments**

474 This study was supported by the National Key Research and Development Program of China (2024YFC2815800,  
475 2023YFC3705503), the National Natural Science Foundation of China (42205103; 42411540229), the Taishan Scholars of  
476 Shandong Province, China (tsqn202306101), the Fundamental Research Funds for the Central Universities (202441011), and

477 the Shandong Provincial Natural Science Foundation (ZR2022QD105). The Fund of Key Laboratory of Marine Ecological  
478 Conservation and Restoration, Ministry of Natural Resources/ Fujian Provincial Key Laboratory of Marine Ecological  
479 Conservation and Restoration (EPR2025009); State Environmental Protection Key Laboratory of Formation and Prevention  
480 of Urban Air Pollution Complex (No. 2025080172).

481 Date and samples were collected onboard of R/V *Dongfanghong 3* and R/V *KeXue* implementing the open research  
482 cruise NORC2024-584 supported by NSFC Shiptime Sharing Project (42349584), the Laoshan Laboratory (LSKJ202201701,  
483 LSKJ202400202), and the Fundamental Research Funds for the Central Universities (202372001, 202472001)

#### 484 Competing interests

485 The authors declare no conflict of interests.

486

#### 487 References

488 Albert, M. F. M. A., Schaap, M., Manders, A. M. M., Scannell, C., O'Dowd, C. D., and de Leeuw, G.: Uncertainties in the  
489 determination of global sub-micron marine organic matter emissions, *Atmospheric Environment*, 57, 289-300,  
490 10.1016/j.atmosenv.2012.04.009, 2012.

491 Aller, J. Y., Radway, J. C., Kilthau, W. P., Bothe, D. W., Wilson, T. W., Vaillancourt, R. D., Quinn, P. K., Coffman, D. J.,  
492 Murray, B. J., and Knopf, D. A.: Size-resolved characterization of the polysaccharidic and proteinaceous components of sea  
493 spray aerosol, *Atmospheric Environment*, 154, 331-347, 10.1016/j.atmosenv.2017.01.053, 2017.

494 Barnes, I., Hjorth, J., and Mihalopoulos, N.: Dimethyl sulfide and dimethyl sulfoxide and their oxidation in the atmosphere,  
495 *Chem. Rev.*, 106, 940-975, 10.1021/cr020529+, 2006.

496 Bates, T. S., Quinn, P. K., Coffman, D. J., Johnson, J. E., Upchurch, L., Saliba, G., Lewis, S., Graff, J., Russell, L. M., and  
497 Behrenfeld, M. J.: Variability in Marine Plankton Ecosystems Are Not Observed in Freshly Emitted Sea Spray Aerosol Over  
498 the North Atlantic Ocean, *Geophys. Res. Lett.*, 47, 10.1029/2019gl085938, 2020.

499 Boreddy, S. K. R., Haque, M. M., and Kawamura, K.: Long-term (2001–2012) trends of carbonaceous aerosols from a  
500 remote island in the western North Pacific: an outflow region of Asian pollutants, *Atmospheric Chemistry and Physics*, 18,  
501 1291-1306, 10.5194/acp-18-1291-2018, 2018.

502 Brooks, S. D. and Thornton, D. C. O.: Marine Aerosols and Clouds, *Annual Review of Marine Science*, 10, 289-313,  
503 10.1146/annurev-marine-121916-063148, 2018a.

504 Brooks, S. D. and Thornton, D. C. O.: Marine Aerosols and Clouds, *Ann Rev Mar Sci*, 10, 289-313, 10.1146/annurev-  
505 marine-121916-063148, 2018b.

506 Bruggemann, M., Hayeck, N., and George, C.: Interfacial photochemistry at the ocean surface is a global source of organic  
507 vapors and aerosols, *Nat Commun*, 9, 2101, 10.1038/s41467-018-04528-7, 2018.

508 Cao, C., Yu, X., Marco Wong, W. H., Sun, N., Zhang, K., Sun, Z., Chen, L., Wu, C., Wang, G., and Yu, J. Z.: An  
509 Instrumental Method for the Simultaneous Determination of Organic Carbon, Elemental Carbon, Inorganic Nitrogen, and  
510 Organic Nitrogen in Aerosol Samples, *J. Geophys. Res. [Atmos.]*, 130, 10.1029/2025jd043904, 2025.

511 Carlton, A. G., Wiedinmyer, C., and Kroll, J. H.: A review of Secondary Organic Aerosol (SOA) formation from isoprene,  
512 *Atmos. Chem. Phys.*, 9, 4987-5005, 10.5194/acp-9-4987-2009, 2009.

513 Cavalli, F.: Advances in characterization of size-resolved organic matter in marine aerosol over the North Atlantic, *J.*  
514 *Geophys. Res.*, 109, D24215, 10.1029/2004jd005137, 2004a.

515 Cavalli, F.: Advances in characterization of size-resolved organic matter in marine aerosol over the North Atlantic, *Journal*  
516 *of Geophysical Research*, 109, 10.1029/2004jd005137, 2004b.

517 Chen, Q., Ikemori, F., and Mochida, M.: Light Absorption and Excitation-Emission Fluorescence of Urban Organic Aerosol  
518 Components and Their Relationship to Chemical Structure, *Environ. Sci. Technol.*, 50, 10859-10868,  
519 10.1021/acs.est.6b02541, 2016a.

520 Chen, Q., Miyazaki, Y., Kawamura, K., Matsumoto, K., Coburn, S., Volkamer, R., Iwamoto, Y., Kagami, S., Deng, Y.,  
521 Ogawa, S., Ramasamy, S., Kato, S., Ida, A., Kajii, Y., and Mochida, M.: Characterization of Chromophoric Water-Soluble  
522 Organic Matter in Urban, Forest, and Marine Aerosols by HR-ToF-AMS Analysis and Excitation-Emission Matrix  
523 Spectroscopy, *Environmental Science & Technology*, 50, 10351-10360, 10.1021/acs.est.6b01643, 2016b.  
524 Chow, J. C., Watson, J. G., Chen, L. W., Arnott, W. P., Moosmuller, H., and Fung, K.: Equivalence of elemental carbon by  
525 thermal/optical reflectance and transmittance with different temperature protocols, *Environ. Sci. Technol.*, 38, 4414-4422,  
526 10.1021/es034936u, 2004.  
527 Christiansen, S., Salter, M. E., Gorokhova, E., Nguyen, Q. T., and Bilde, M.: Sea spray aerosol formation: Laboratory results  
528 on the role of air entrainment, water temperature, and phytoplankton biomass, *Environ. Sci. Technol.*, 53, 13107-13116,  
529 10.1021/acs.est.9b04078, 2019.  
530 Cochran, R. E., Laskina, O., Jayarathne, T., Laskin, A., Laskin, J., Lin, P., Sultana, C., Lee, C., Moore, K. A., Cappa, C. D.,  
531 Bertram, T. H., Prather, K. A., Grassian, V. H., and Stone, E. A.: Analysis of Organic Anionic Surfactants in Fine and  
532 Coarse Fractions of Freshly Emitted Sea Spray Aerosol, *Environmental Science & Technology*, 50, 2477-2486,  
533 10.1021/acs.est.5b04053, 2016a.  
534 Cochran, R. E., Laskina, O., Jayarathne, T., Laskin, A., Laskin, J., Lin, P., Sultana, C., Lee, C., Moore, K. A., Cappa, C. D.,  
535 Bertram, T. H., Prather, K. A., Grassian, V. H., and Stone, E. A.: Analysis of Organic Anionic Surfactants in Fine and  
536 Coarse Fractions of Freshly Emitted Sea Spray Aerosol, *Environ. Sci. Technol.*, 50, 2477-2486, 10.1021/acs.est.5b04053,  
537 2016b.  
538 Cochran, R. E., Laskina, O., Trueblood, J. V., Estillore, A. D., Morris, H. S., Jayarathne, T., Sultana, C. M., Lee, C., Lin, P.,  
539 Laskin, J., Laskin, A., Dowling, J. A., Qin, Z., Cappa, C. D., Bertram, T. H., Tivanski, A. V., Stone, E. A., Prather, K. A.,  
540 and Grassian, V. H.: Molecular Diversity of Sea Spray Aerosol Particles: Impact of Ocean Biology on Particle Composition  
541 and Hygroscopicity, *Chem*, 2, 655-667, 10.1016/j.chempr.2017.03.007, 2017.  
542 Cravagan, L. T., Mallet, M. D., Vaattovaara, P., Harvey, M. J., Law, C. S., Modini, R. L., Russell, L. M., Stelcer, E., Cohen,  
543 D. D., Olsen, G., Safi, K., Burrell, T. J., and Ristovski, Z.: Sea spray aerosol organic enrichment, water uptake and surface  
544 tension effects, *Atmospheric Chemistry and Physics*, 20, 7955-7977, 10.5194/acp-20-7955-2020, 2020.  
545 Crocker, D. R., Kaluarachchi, C. P., Cao, R., Dinasquet, J., Franklin, E. B., Morris, C. K., Amiri, S., Petras, D., Nguyen, T.,  
546 Torres, R. R., Martz, T. R., Malfatti, F., Goldstein, A. H., Tivanski, A. V., Prather, K. A., and Thiemens, M. H.: Isotopic  
547 Insights into Organic Composition Differences between Supermicron and Submicron Sea Spray Aerosol, *Environmental  
548 Science & Technology*, 56, 9947-9958, 10.1021/acs.est.2c02154, 2022.  
549 Cui, L., Xiao, Y., Hu, W., Song, L., Wang, Y., Zhang, C., Fu, P., and Zhu, J.: Enhanced dataset of global marine isoprene  
550 emissions from biogenic and photochemical processes for the period 2001–2020, *Earth System Science Data*, 15, 5403-5425,  
551 10.5194/essd-15-5403-2023, 2023.  
552 de Jonge, R. W., Xavier, C., Olenius, T., Elm, J., Svenhag, C., Hyttinen, N., Nieradzik, L., Sarnela, N., Kristensson, A.,  
553 Petaja, T., Ehn, M., and Roldin, P.: Natural Marine Precursors Boost Continental New Particle Formation and Production of  
554 Cloud Condensation Nuclei, *Environmental Science & Technology*, 58, 10956-10968, 10.1021/acs.est.4c01891, 2024.  
555 de Leeuw, G., Andreas, E. L., Anguelova, M. D., Fairall, C. W., Lewis, E. R., O'Dowd, C., Schulz, M., and Schwartz, S. E.:  
556 Production flux of sea spray aerosol, *Rev. Geophys.*, 49, 10.1029/2010rg000349, 2011.  
557 DeMott, P. J., Hill, T. C., McCluskey, C. S., Prather, K. A., Collins, D. B., Sullivan, R. C., Ruppel, M. J., Mason, R. H., Irish,  
558 V. E., Lee, T., Hwang, C. Y., Rhee, T. S., Snider, J. R., McMeeking, G. R., Dhaniyala, S., Lewis, E. R., Wentzell, J. J.,  
559 Abbatt, J., Lee, C., Sultana, C. M., Ault, A. P., Axson, J. L., Diaz Martinez, M., Venero, I., Santos-Figueroa, G., Stokes, M.  
560 D., Deane, G. B., Mayol-Bracero, O. L., Grassian, V. H., Bertram, T. H., Bertram, A. K., Moffett, B. F., and Franc, G. D.:  
561 Sea spray aerosol as a unique source of ice nucleating particles, *The Proceedings of the National Academy of Sciences*, 113,  
562 5797-5803, 10.1073/pnas.1514034112, 2016.  
563 Facchini, M. C., Rinaldi, M., Decesari, S., Carbone, C., Finessi, E., Mircea, M., Fuzzi, S., Ceburnis, D., Flanagan, R.,  
564 Nilsson, E. D., de Leeuw, G., Martino, M., Woeltjen, J., and O'Dowd, C. D.: Primary submicron marine aerosol dominated  
565 by insoluble organic colloids and aggregates, *Geophys. Res. Lett.*, 35, 10.1029/2008gl034210, 2008.  
566 Fu, P., Kawamura, K., and Miura, K.: Molecular characterization of marine organic aerosols collected during a round-the-  
567 world cruise, *Journal of Geophysical Research*, 116, 10.1029/2011jd015604, 2011.

568 Fu, P., Kawamura, K., Chen, J., Qin, M., Ren, L., Sun, Y., Wang, Z., Barrie, L. A., Tachibana, E., Ding, A., and Yamashita,  
569 Y.: Fluorescent water-soluble organic aerosols in the High Arctic atmosphere, *Scientific Reports*, 5, 9845,  
570 10.1038/srep09845, 2015.

571 Gant, B. and Meskhidze, N.: The physical and chemical characteristics of marine primary organic aerosol: a review,  
572 *Atmospheric Chemistry and Physics*, 13, 3979-3996, 10.5194/acp-13-3979-2013, 2013.

573 Gant, B., Meskhidze, N., Facchini, M. C., Rinaldi, M., Ceburnis, D., and O'Dowd, C. D.: Wind speed dependent size-  
574 resolved parameterization for the organic mass fraction of sea spray aerosol, *Atmos. Chem. Phys.*, 11, 8777-8790,  
575 10.5194/acp-11-8777-2011, 2011.

576 Gant, B., Johnson, M. S., Meskhidze, N., Sciare, J., Ovadnevaite, J., Ceburnis, D., and O'Dowd, C. D.: Model evaluation of  
577 marine primary organic aerosol emission schemes, *Atmos. Chem. Phys.*, 12, 8553-8566, 10.5194/acp-12-8553-2012, 2012.

578 Gruber, E. R. and Rudich, Y.: Atmospheric HULIS: How humic-like are they? A comprehensive and critical review, *Atmos.*  
579 *Chem. Phys.*, 6, 729-753, 10.5194/acp-6-729-2006, 2006.

580 Grythe, H., Ström, J., Krejci, R., Quinn, P., and Stohl, A.: A review of sea-spray aerosol source functions using a large  
581 global set of sea salt aerosol concentration measurements, *Atmospheric Chemistry and Physics*, 14, 1277-1297, 10.5194/acp-  
582 14-1277-2014, 2014.

583 Gu, W., Xie, Z., Wei, Z., Chen, A., Jiang, B., Yue, F., and Yu, X.: Marine Fresh Carbon Pool Dominates Summer  
584 Carbonaceous Aerosols Over Arctic Ocean, *J. Geophys. Res., [Atmos.]*, 128, 10.1029/2022jd037692, 2023.

585 Gupta, M., Sahu, L. K., Tripathi, N., Sudheer, A. K., and Singh, A.: Processes Controlling DMS Variability in Marine  
586 Boundary Layer of the Arabian Sea During Post-Monsoon Season of 2021, *J. Geophys. Res., [Atmos.]*, 130,  
587 10.1029/2024jd042547, 2025.

588 Hedges, J. I.: Global biogeochemical cycles: progress and problems, *Marine Chemistry*, 39, 67-93,  
589 [https://doi.org/10.1016/0304-4203\(92\)90096-S](https://doi.org/10.1016/0304-4203(92)90096-S), 1992.

590 Hersbach, H., Bell, B., Berrisford, P., Hirahara, S., Horányi, A., Muñoz-Sabater, J., Nicolas, J., Peubey, C., Radu, R.,  
591 Schepers, D., Simmons, A., Soci, C., Abdalla, S., Abellán, X., Balsamo, G., Bechtold, P., Biavati, G., Bidlot, J., Bonavita,  
592 M., De Chiara, G., Dahlgren, P., Dee, D., Diamantakis, M., Dragani, R., Flemming, J., Forbes, R., Fuentes, M., Geer, A.,  
593 Haimberger, L., Healy, S., Hogan, R. J., Hólm, E., Janisková, M., Keeley, S., Laloyaux, P., Lopez, P., Lupu, C., Radnoti, G.,  
594 de Rosnay, P., Rozum, I., Vamborg, F., Villaume, S., and Thépaut, J. N.: The ERA5 global reanalysis, *Quarterly Journal of*  
595 *the Royal Meteorological Society*, 146, 1999-2049, 10.1002/qj.3803, 2020.

596 Hoque, M., Kawamura, K., Seki, O., and Hoshi, N.: Spatial distributions of dicarboxylic acids,  $\omega$ -oxoacids, pyruvic acid and  
597  $\alpha$ -dicarbonyls in the remote marine aerosols over the North Pacific, *Marine Chemistry*, 172, 1-11,  
598 10.1016/j.marchem.2015.03.003, 2015.

599 Hoque, M. M. M., Kawamura, K., and Uematsu, M.: Spatio-temporal distributions of dicarboxylic acids,  $\omega$ -oxocarboxylic  
600 acids, pyruvic acid,  $\alpha$ -dicarbonyls and fatty acids in the marine aerosols from the North and South Pacific, *Atmospheric*  
601 *Research*, 185, 158-168, 10.1016/j.atmosres.2016.10.022, 2017.

602 Hsu, S.-C., Wong, G. T. F., Gong, G.-C., Shiah, F.-K., Huang, Y.-T., Kao, S.-J., Tsai, F., Candice Lung, S.-C., Lin, F.-J., Lin,  
603 I. I., Hung, C.-C., and Tseng, C.-M.: Sources, solubility, and dry deposition of aerosol trace elements over the East China  
604 Sea, *Mar. Chem.*, 120, 116-127, 10.1016/j.marchem.2008.10.003, 2010.

605 Hu, J., Li, J., Tsoma Tchinda, N., Song, Y., Xu, M., Li, K., and Du, L.: Underestimated role of sea surface temperature in sea  
606 spray aerosol formation and climate effects, *npj Climate and Atmospheric Science*, 7, 10.1038/s41612-024-00823-x, 2024.

607 Huang, S., Wu, Z., Poulain, L., van Pinxteren, M., Merkel, M., Assmann, D., Herrmann, H., and Wiedensohler, A.: Source  
608 apportionment of the organic aerosol over the Atlantic Ocean from 53° N to 53° S: significant contributions from marine  
609 emissions and long-range transport, *Atmos. Chem. Phys.*, 18, 18043-18062, 10.5194/acp-18-18043-2018, 2018.

610 Huang, S., Wu, Z., Wang, Y., Poulain, L., Hopner, F., Merkel, M., Herrmann, H., and Wiedensohler, A.: Aerosol  
611 Hygroscopicity and its Link to Chemical Composition in a Remote Marine Environment Based on Three Transatlantic  
612 Measurements, *Environmental Science & Technology*, 56, 9613-9622, 10.1021/acs.est.2c00785, 2022.

613 Huebert, B. J. and Charlson, R. J.: Uncertainties in data on organic aerosols, *Tellus B: Chemical and Physical Meteorology*,  
614 52, 10.3402/tellusb.v52i5.17099, 2000.

615 Kunwar, B. and Kawamura, K.: One-year observations of carbonaceous and nitrogenous components and major ions in the  
616 aerosols from subtropical Okinawa Island, an outflow region of Asian dusts, *Atmos. Chem. Phys.*, 14, 1819-1836,  
617 10.5194/acp-14-1819-2014, 2014.

618 Laskin, A., Laskin, J., and Nizkorodov, S. A.: Chemistry of atmospheric brown carbon, *Chem. Rev.*, 115, 4335-4382,  
619 10.1021/cr5006167, 2015.

620 Lawler, M. J., Lewis, S. L., Russell, L. M., Quinn, P. K., Bates, T. S., Coffman, D. J., Upchurch, L. M., and Saltzman, E. S.:  
621 North Atlantic marine organic aerosol characterized by novel offline thermal desorption mass spectrometry: polysaccharides,  
622 recalcitrant material, and secondary organics, *Atmospheric Chemistry and Physics*, 20, 16007-16022, 10.5194/acp-20-  
623 16007-2020, 2020.

624 Lewis, E. and Schwartz, S.: Sea Salt Aerosol Production: Mechanisms, Methods, Measurements and Models—A Critical  
625 Review, Washington DC American Geophysical Union Geophysical Monograph Series, 152, 3719, 10.1029/GM152, 2004.

626 Li, J., Han, Z., Fu, P., Yao, X., and Liang, M.: Seasonal characteristics of emission, distribution, and radiative effect of  
627 marine organic aerosols over the western Pacific Ocean: an investigation with a coupled regional climate aerosol model,  
628 *Atmospheric Chemistry and Physics*, 24, 3129-3161, 10.5194/acp-24-3129-2024, 2024.

629 Lim, H. J. and Turpin, B. J.: Origins of primary and secondary organic aerosol in Atlanta: results of time-resolved  
630 measurements during the Atlanta Supersite Experiment, *Environ. Sci. Technol.*, 36, 4489-4496, 10.1021/es0206487, 2002.

631 Ma, X., Li, K., Zhang, S., Tchinda, N. T., Li, J., Herrmann, H., and Du, L.: Molecular characteristics of sea spray aerosols  
632 during aging with the participation of marine volatile organic compounds, *Science of the Total Environment*, 954, 176380,  
633 10.1016/j.scitotenv.2024.176380, 2024.

634 Miyazaki, Y., Kawamura, K., and Sawano, M.: Size distributions and chemical characterization of water-soluble organic  
635 aerosols over the western North Pacific in summer, *Journal of Geophysical Research: Atmospheres*, 115,  
636 10.1029/2010jd014439, 2010.

637 Miyazaki, Y., Suzuki, K., Tachibana, E., Yamashita, Y., Muller, A., Kawana, K., and Nishioka, J.: New index of organic  
638 mass enrichment in sea spray aerosols linked with senescent status in marine phytoplankton, *Scientific Reports*, 10, 17042,  
639 10.1038/s41598-020-73718-5, 2020.

640 Miyazaki, Y., Yamashita, Y., Kawana, K., Tachibana, E., Kagami, S., Mochida, M., Suzuki, K., and Nishioka, J.: Chemical  
641 transfer of dissolved organic matter from surface seawater to sea spray water-soluble organic aerosol in the marine  
642 atmosphere, *Scientific Reports*, 8, 14861, 10.1038/s41598-018-32864-7, 2018a.

643 Miyazaki, Y., Yamashita, Y., Kawana, K., Tachibana, E., Kagami, S., Mochida, M., Suzuki, K., and Nishioka, J.: Chemical  
644 transfer of dissolved organic matter from surface seawater to sea spray water-soluble organic aerosol in the marine  
645 atmosphere, *Sci. Rep.*, 8, 14861, 10.1038/s41598-018-32864-7, 2018b.

646 Murphy, K. R., Stedmon, C. A., Graeber, D., and Bro, R.: Fluorescence spectroscopy and multi-way techniques. PARAFAC,  
647 Analytical Methods, 5, 10.1039/c3ay41160e, 2013.

648 O'Dowd, C. D., Langmann, B., Varghese, S., Scannell, C., Ceburnis, D., and Facchini, M. C.: A combined organic-inorganic  
649 sea-spray source function, *Geophysical Research Letters*, 35, 10.1029/2007gl030331, 2008.

650 O'Dowd, C. D., Facchini, M. C., Cavalli, F., Ceburnis, D., Mircea, M., Decesari, S., Fuzzi, S., Yoon, Y. J., and Putaud, J. P.:  
651 Biogenically driven organic contribution to marine aerosol, *Nature*, 431, 676-680, 10.1038/nature02959, 2004.

652 Pöhlker, C., Huffman, J. A., and Pöschl, U.: Autofluorescence of atmospheric bioaerosols – fluorescent biomolecules and  
653 potential interferences, *Atmos. Meas. Tech.*, 5, 37-71, 10.5194/amt-5-37-2012, 2012.

654 Prather, K. A., Bertram, T. H., Grassian, V. H., Deane, G. B., Stokes, M. D., Demott, P. J., Aluwihare, L. I., Palenik, B. P.,  
655 Azam, F., Seinfeld, J. H., Moffet, R. C., Molina, M. J., Cappa, C. D., Geiger, F. M., Roberts, G. C., Russell, L. M., Ault, A.  
656 P., Baltrusaitis, J., Collins, D. B., Corrigan, C. E., Cuadra-Rodriguez, L. A., Ebbin, C. J., Forestieri, S. D., Guasco, T. L.,  
657 Hersey, S. P., Kim, M. J., Lambert, W. F., Modini, R. L., Mui, W., Pedler, B. E., Ruppel, M. J., Ryder, O. S., Schoepp, N. G.,  
658 Sullivan, R. C., and Zhao, D.: Bringing the ocean into the laboratory to probe the chemical complexity of sea spray aerosol,  
659 *Proc. Natl. Acad. Sci. USA*, 110, 7550-7555, 10.1073/pnas.1300262110, 2013.

660 Quinn, P. K. and Bates, T. S.: The case against climate regulation via oceanic phytoplankton sulphur emissions, *Nature*, 480,  
661 51-56, 10.1038/nature10580, 2011.

662 Quinn, P. K., Coffman, D. J., Johnson, J. E., Upchurch, L. M., and Bates, T. S.: Small fraction of marine cloud condensation  
663 nuclei made up of sea spray aerosol, *Nat. Geosci.*, 10, 674-679, 10.1038/ngeo3003, 2017.

664 Quinn, P. K., Collins, D. B., Grassian, V. H., Prather, K. A., and Bates, T. S.: Chemistry and related properties of freshly  
665 emitted sea spray aerosol, *Chem. Rev.*, 115, 4383-4399, 10.1021/cr500713g, 2015a.

666 Quinn, P. K., Collins, D. B., Grassian, V. H., Prather, K. A., and Bates, T. S.: Chemistry and related properties of freshly  
667 emitted sea spray aerosol, *Chemical Review*, 115, 4383-4399, 10.1021/cr500713g, 2015b.

668 Quinn, P. K., Bates, T. S., Schulz, K. S., Coffman, D. J., Frossard, A. A., Russell, L. M., Keene, W. C., and Kieber, D. J.:  
669 Contribution of sea surface carbon pool to organic matter enrichment in sea spray aerosol, *Nat. Geosci.*, 7, 228-232,  
670 10.1038/ngeo2092, 2014.

671 Rinaldi, M., Fuzzi, S., Decesari, S., Marullo, S., Santoleri, R., Provenzale, A., von Hardenberg, J., Ceburnis, D., Vaishya, A.,  
672 O'Dowd, C. D., and Facchini, M. C.: Is chlorophyll-athe best surrogate for organic matter enrichment in submicron primary  
673 marine aerosol?, *Journal of Geophysical Research: Atmospheres*, 118, 4964-4973, 10.1002/jgrd.50417, 2013.

674 Russell, L. M., Hawkins, L. N., Frossard, A. A., Quinn, P. K., and Bates, T. S.: Carbohydrate-like composition of submicron  
675 atmospheric particles and their production from ocean bubble bursting, *The Proceedings of the National Academy of  
676 Sciences* 107, 6652-6657, 10.1073/pnas.0908905107, 2010.

677 Sahu, L. K., Kondo, Y., Miyazaki, Y., Kuwata, M., Koike, M., Takegawa, N., Tanimoto, H., Matsueda, H., Yoon, S. C., and  
678 Kim, Y. J.: Anthropogenic aerosols observed in Asian continental outflow at Jeju Island, Korea, in spring 2005, *J. Geophys.  
679 Res., [Atmos.]*, 114, 10.1029/2008jd010306, 2009.

680 Salter, M. E., Nilsson, E. D., Butcher, A., and Bilde, M.: On the seawater temperature dependence of the sea spray aerosol  
681 generated by a continuous plunging jet, *Journal of Geophysical Research: Atmospheres*, 119, 9052-9072,  
682 10.1002/2013jd021376, 2014.

683 Santander, M. V., Schiffer, J. M., Lee, C., Axson, J. L., Tauber, M. J., and Prather, K. A.: Factors controlling the transfer of  
684 biogenic organic species from seawater to sea spray aerosol, *Scientific Reports*, 12, 3580, 10.1038/s41598-022-07335-9,  
685 2022.

686 Santander, M. V., Mitts, B. A., Pendergraft, M. A., Dinasquet, J., Lee, C., Moore, A. N., Cancelada, L. B., Kimble, K. A.,  
687 Malfatti, F., and Prather, K. A.: Tandem Fluorescence Measurements of Organic Matter and Bacteria Released in Sea Spray  
688 Aerosols, *Environmental Science & Technology*, 55, 5171-5179, 10.1021/acs.est.0c05493, 2021.

689 Schmitt-Kopplin, P., Liger-Belair, G., Koch, B. P., Flerus, R., Kattner, G., Harir, M., Kanawati, B., Lucio, M., Tziotis, D.,  
690 Hertkorn, N., and Gebefügi, I.: Dissolved organic matter in sea spray: a transfer study from marine surface water to aerosols,  
691 *Biogeosciences*, 9, 1571-1582, 10.5194/bg-9-1571-2012, 2012.

692 Shank, L. M., Howell, S., Clarke, A. D., Freitag, S., Brekhovskikh, V., Kapustin, V., McNaughton, C., Campos, T., and  
693 Wood, R.: Organic matter and non-refractory aerosol over the remote Southeast Pacific: oceanic and combustion sources,  
694 *Atmos. Chem. Phys.*, 12, 557-576, 10.5194/acp-12-557-2012, 2012.

695 Siemer, J. P., Machín, F., González-Vega, A., Arrieta, J. M., Gutiérrez-Guerra, M. A., Pérez-Hernández, M. D., Vélez-Belchí,  
696 P., Hernández-Guerra, A., and Fraile-Nuez, E.: Recent Trends in SST, Chl-a, Productivity and Wind Stress in Upwelling and  
697 Open Ocean Areas in the Upper Eastern North Atlantic Subtropical Gyre, *J. Geophys. Res., [Oceans]*, 126,  
698 10.1029/2021jc017268, 2021.

699 Sinclair, K., van Diedenhoven, B., Cairns, B., Alexandrov, M., Moore, R., Ziomba, L. D., and Crosbie, E.: Observations of  
700 Aerosol-Cloud Interactions During the North Atlantic Aerosol and Marine Ecosystem Study, *Geophysical Research Letters*,  
701 47, 10.1029/2019gl085851, 2020.

702 Spracklen, D. V., Arnold, S. R., Sciare, J., Carslaw, K. S., and Pio, C.: Globally significant oceanic source of organic carbon  
703 aerosol, *Geophys. Res. Lett.*, 35, 10.1029/2008gl033359, 2008.

704 Stedmon, C. A. and Bro, R.: Characterizing dissolved organic matter fluorescence with parallel factor analysis: a tutorial,  
705 *Limnology and Oceanography: Methods*, 6, 572-579, 10.4319/lom.2008.6.572, 2008.

706 Tang, J., Xu, B., Zhao, S., Li, J., Tian, L., Geng, X., Jiang, H., Mo, Y., Zhong, G., Jiang, B., Chen, Y., Tang, J., and Zhang,  
707 G.: Long-Emission-Wavelength Humic-Like Component (L-HULIS) as a Secondary Source Tracer of Brown Carbon in the  
708 Atmosphere, *Journal of Geophysical Research: Atmospheres*, 129, 10.1029/2023jd040144, 2024.

709 Tripathi, N., Girach, I. A., Kompalli, S. K., Murari, V., Nair, P. R., Babu, S. S., and Sahu, L. K.: Sources and Distribution of  
710 Light NMHCs in the Marine Boundary Layer of the Northern Indian Ocean During Winter: Implications to Aerosol  
711 Formation, *J. Geophys. Res., [Atmos.]*, 129, 10.1029/2023jd039433, 2024.

712 Tripathi, N., Sahu, L. K., Singh, A., Yadav, R., Patel, A., Patel, K., and Meenu, P.: Elevated Levels of Biogenic Nonmethane  
713 Hydrocarbons in the Marine Boundary Layer of the Arabian Sea During the Intermonsoon, *J. Geophys. Res., [Atmos.]*, 125,  
714 10.1029/2020jd032869, 2020.

715 Trueblood, J. V., Wang, X., Or, V. W., Alves, M. R., Santander, M. V., Prather, K. A., and Grassian, V. H.: The Old and the  
716 New: Aging of Sea Spray Aerosol and Formation of Secondary Marine Aerosol through OH Oxidation Reactions, *ACS  
717 Earth and Space Chemistry*, 3, 2307-2314, 10.1021/acsearthspacechem.9b00087, 2019.

718 Tuchen, F. P., Perez, R. C., Foltz, G. R., Brandt, P., Subramaniam, A., Lee, S. K., Lumpkin, R., and Hummels, R.:  
719 Modulation of Equatorial Currents and Tropical Instability Waves During the 2021 Atlantic Niño, *J. Geophys. Res.,*  
720 [Oceans], 129, 10.1029/2023jc020431, 2023.

721 Turpin, B. J. and Huntzicker, J. J.: Identification of Secondary Organic Aerosol Episodes and Quantitation of Primary and  
722 Secondary Organic Aerosol Concentrations During SCAQS, *Atmospheric Environment*, 29, 3527-3544, 10.1016/1352-  
723 2310(94)00276-Q, 1995.

724 Vergara-Temprado, J., Murray, B. J., Wilson, T. W., O'Sullivan, D., Browse, J., Pringle, K. J., Ardon-Dryer, K., Bertram, A.  
725 K., Burrows, S. M., Ceburnis, D., DeMott, P. J., Mason, R. H., O'Dowd, C. D., Rinaldi, M., and Carslaw, K. S.: Contribution  
726 of feldspar and marine organic aerosols to global ice nucleating particle concentrations, *Atmospheric Chemistry and Physics*,  
727 17, 3637-3658, 10.5194/acp-17-3637-2017, 2017.

728 Vignati, E., Facchini, M. C., Rinaldi, M., Scannell, C., Ceburnis, D., Sciare, J., Kanakidou, M., Myriokefalitakis, S.,  
729 Dentener, F., and O'Dowd, C. D.: Global scale emission and distribution of sea-spray aerosol: Sea-salt and organic  
730 enrichment, *Atmos. Environ.*, 44, 670-677, 10.1016/j.atmosenv.2009.11.013, 2010.

731 Wang, J., Zhang, H. H., Booge, D., Zhang, Y. Q., Li, X. J., Wu, Y. C., Zhang, J. W., and Chen, Z. H.: Isoprene Production  
732 and Its Driving Factors in the Northwest Pacific Ocean, *Global Biogeochem. Cy.*, 37, 10.1029/2023gb007841, 2023a.

733 Wang, X., Deane, G. B., Moore, K. A., Ryder, O. S., Stokes, M. D., Beall, C. M., Collins, D. B., Santander, M. V., Burrows,  
734 Sultana, C. M., and Prather, K. A.: The role of jet and film drops in controlling the mixing state of submicron sea  
735 spray aerosol particles, *Proc. Natl. Acad. Sci. USA*, 114, 6978-6983, 10.1073/pnas.1702420114, 2017.

736 Wang, X., Sultana, C. M., Trueblood, J., Hill, T. C., Malfatti, F., Lee, C., Laskina, O., Moore, K. A., Beall, C. M.,  
737 McCluskey, C. S., Cornwell, G. C., Zhou, Y., Cox, J. L., Pendergraft, M. A., Santander, M. V., Bertram, T. H., Cappa, C. D.,  
738 Azam, F., DeMott, P. J., Grassian, V. H., and Prather, K. A.: Microbial Control of Sea Spray Aerosol Composition: A Tale  
739 of Two Blooms, *ACS Central Science*, 1, 124-131, 10.1021/acscentsci.5b00148, 2015.

740 Wang, Y., Zhang, P., Li, J., Liu, Y., Zhang, Y., Li, J., and Han, Z.: An updated aerosol simulation in the Community Earth  
741 System Model (v2.1.3): dust and marine aerosol emissions and secondary organic aerosol formation, *Geoscientific Model  
742 Development*, 17, 7995-8021, 10.5194/gmd-17-7995-2024, 2024.

743 Wang, Y., Zhang, Y., Li, W., Wu, G., Qi, Y., Li, S., Zhu, W., Yu, J. Z., Yu, X., Zhang, H. H., Sun, J., Wang, W., Sheng, L.,  
744 Yao, X., Gao, H., Huang, C., Ma, Y., and Zhou, Y.: Important roles and formation of atmospheric organosulfates in marine  
745 organic aerosols: Influence of phytoplankton emissions and anthropogenic pollutants, *Environ. Sci. Technol.*, 57, 10284-  
746 10294, 10.1021/acs.est.3c01422, 2023b.

747 Wolf, M. J., Coe, A., Dove, L. A., Zawadowicz, M. A., Dooley, K., Biller, S. J., Zhang, Y., Chisholm, S. W., and Cziczo, D.  
748 J.: Investigating the Heterogeneous Ice Nucleation of Sea Spray Aerosols Using Prochlorococcus as a Model Source of  
749 Marine Organic Matter, *Environmental Science & Technology*, 53, 1139-1149, 10.1021/acs.est.8b05150, 2019.

750 Xu, W., Ovadnevaite, J., Fossum, K. N., Lin, C., Huang, R.-J., Ceburnis, D., and O'Dowd, C.: Sea spray as an obscured  
751 source for marine cloud nuclei, *Nature Geoscience*, 15, 282-286, 10.1038/s41561-022-00917-2, 2022.

752 Yu, Y., Wang, H., Wang, T., Song, K., Tan, T., Wan, Z., Gao, Y., Dong, H., Chen, S., Zeng, L., Hu, M., Wang, H., Lou, S.,  
753 Zhu, W., and Guo, S.: Elucidating the importance of semi-volatile organic compounds to secondary organic aerosol  
754 formation at a regional site during the EXPLORE-YRD campaign, *Atmos. Environ.*, 246, 10.1016/j.atmosenv.2020.118043,  
755 2021.

756 Yu, Z. and Li, Y.: Marine volatile organic compounds and their impacts on marine aerosol-A review, *Sci. Total Environ.*,  
757 768, 145054, 10.1016/j.scitotenv.2021.145054, 2021.

758 Zhang, W. and Gu, D.: Geostationary satellite reveals increasing marine isoprene emissions in the center of the equatorial  
759 Pacific Ocean, *npj Climate and Atmospheric Science*, 5, 1, 10.1038/s41612-022-00311-0, 2022.

760 Zhang, Y., Wang, Y., Li, S., Yi, Y., Guo, Y., Yu, C., Jiang, Y., Ni, Y., Hu, W., Zhu, J., Qi, J., Shi, J., Yao, X., and Gao, H.:  
761 Sources and Optical Properties of Marine Organic Aerosols Under the Influence of Marine Emissions, Asian Dust, and  
762 Anthropogenic Pollutants, *J. Geophys. Res., [Atmos.]*, 130, 10.1029/2025jd043472, 2025.

763 Zhao, X., Liu, X., Burrows, S. M., and Shi, Y.: Effects of marine organic aerosols as sources of immersion-mode ice-  
764 nucleating particles on high-latitude mixed-phase clouds, *Atmospheric Chemistry and Physics*, 21, 2305-2327, 10.5194/acp-  
765 21-2305-2021, 2021.

766

767